Charts of spatial noise distribution in planer resistors with finite contacts

th e

CHARTS OF SPATIAL NOISE
DISTRIBUTION IN PLANAR RESISTORS
WITH FINITE CONTACTS

by

A.H. de Kuijper and L.K.J. Vandamme

E I N D H O V E N U N I V E R S I T Y O F T E C H N O L O G Y

Department of Electrical Engineering

Eindhoven The Netherlands

CHARTS OF SPATIAL NOISE DISTRIBUTION IN PLANAR RESISTORS WITH FINITE CONTACTS

by

A.H. de Kuijper

and

L.K.J. Vandamme

TH-Report 79-E-94

ISBN 90-6144-094-7

Eindhoven

January 1979

CHARTS OF SPATIAL NOISE DISTRIBUTION IN PLANAR RESISTORS WITH FINITE CONTACTS

A.H. de Kuijper and L.K.J. Vandamme,
Eindhoven University of Technology,
Department of Electrical Engineering,
Eindhoven, Netherlands.

Abstract

Calculations and experimental results are presented of the voltage and the voltage fluctuations across a pair of sensor electrodes on a planar resistor. A constant current is passed through another pair of driver electrodes. Three types of geometry are considered all of which are invariant for rotations of 90 degrees. Areas of low and high contributions to the voltage fluctuations are calculated assuming homogeneous conductivity fluctuations. Sixty-six spatial noise distribution charts are presented. The noise parameter of conductance fluctuations in films can be calculated from experimental results under different measuring conditions and for different geometries.
The calculation method rests on the sensitivity theorem in electrical network. Calculations are in agreement with experimental results.

Introduction

A general expression has been derived for the spectral noise density of the voltage fluctuations between two arbitrarily shaped sensor electrodes placed arbitrarily on a two-dimensional conductor for the case that a constant current is applied to another pair of arbitrarily shaped and positioned driver electrodes [1,2].
The current is assumed to be noise-free. The voltage fluctuations across the sensor electrodes are caused by homogeneous resistivity fluctuations. This report comprises calculations with regard to the noise and the noise distribution in two-dimensional conductors with a geometry as shown in Figs. 1a, 1b and 1c.

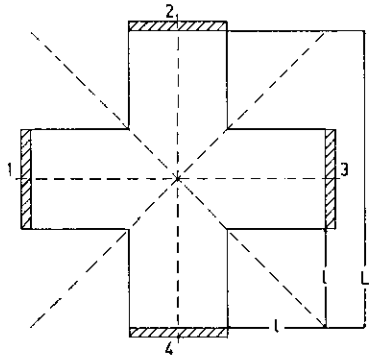

Fig. 1a

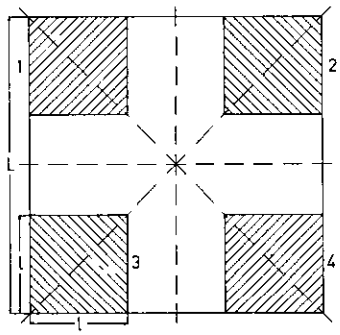

Fig. 1b

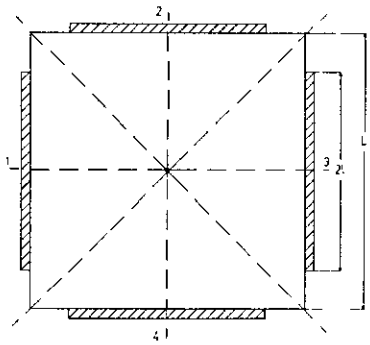

Fig. 1c

All figures: ///// : ideal contacts

Fig. 1a: Cross-shaped planar resistor with 4 contacts.
Fig. 1b: Square-shaped planar resistor with 4 corner contacts.
Fig. 1c: Square-shaped planar resistor with 4 side contacts.

The samples are invariant for rotations of 90 degrees. We calculated the noise power at the sensor electrodes and the spatial noise distribution for various $2l/L$ ratios and various connections of the current source and sensor to the contacts. The noise consists of a thermal noise term and a conduction noise term. The thermal noise is proportional to the resistance between the sensor electrodes. When a constant current is passed through the sample, the conductivity fluctuations cause electric field fluctuations, which can be observed either on the sensor electrodes, the driver electrodes or across one driver and one sensor electrode. The conduction noise term is proportional

to the square of the current I passed through the sample.
Here we consider noise due to conductivity fluctuations.

1. Calculation of the noise power density S_V.

We assume the material to be homogeneous. The statistical properties of the conductivity fluctuations are also assumed to be homogeneous. The driver and sensor electrodes are assumed to be ideally conducting. The calculations have been developed from a purely macroscopic point of view without any reference to the origin and particular properties of the spectrum of the conductance fluctuations.
To obtain numerical results we carried out calculations on a network that simulated a two-dimensional conductor. This network consists of horizontal and vertical resistors, all having the same value, a current source and resistors to simulate the contacts. The current source was connected to a pair of driver electrodes D, and the voltage fluctuations were calculated on a pair of sensor electrodes Q. The first order sensitivity $\delta V_Q/\delta R$ was calculated by using the adjoint network [3,4]. In our case the adjoint network was obtained only by changing sensor and driver electrodes.
The sensitivity of the voltage changes across the sensors in the original network due to a small change in a resistor R at an arbitrary place in the network is then given by the first order sensitivity

$$\frac{\delta V_Q}{\delta R} = \frac{i\tilde{i}}{I} \qquad (1)$$

where i is the current through that resistor in the original network, $\tilde{i}$ is the current through the same resistor in the adjoint network and I is 1A. We shall only consider the first-order sensitivities given by (1). $\delta V_Q/\delta R$ is proportional to I, because i and $\tilde{i}$ are proportional to I.
To calculate the total squared average voltage fluctuations $\langle(\delta V_Q)^2\rangle$, we devides the network in equal squares, each having the same properties in the x and y directions. Fig. 2 gives some possibilities of connecting the resistors inside such squares.
The possibilities denoted by 2 and 3 inside the dotted line in fig. 2 have the drawbacks that they strongly increase the number of nodes and the number of resistors. Therefore, we chose the representation denoted by 1 and called it the "L-form" square of unit area. In ref. [1] it is demonstrated that the total average of the squared voltage fluctuations $\langle(\delta V_Q)^2\rangle$ is

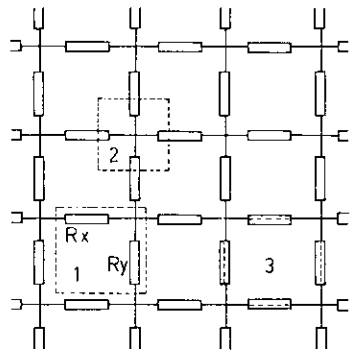

Fig. 2: The lumped network model of a planar resistor showing three possible representations of a unit area A by resistors.

$$\langle(\Delta V_Q)^2\rangle = \frac{\langle(\Delta R)^2\rangle}{I^2} \sum_{\substack{\text{all}\\ \text{squares}}} [i_x \tilde{i}_x + i_y \tilde{i}_y]^2 \qquad (2)$$

where i_x, i_x and $i_y, \tilde{i}_y$ are the currents and adjoints currents through R_x and R_y of an "L-form" area. $\langle(\Delta R)^2\rangle$ stands for the variance of the resistance fluctuations in R_x and R_y. The sum in (2) must be taken over all squares of the network. Since the network is purely resistive, the method applies to frequency as well as time domain calculations. The spectral noise power density S_Q is the variance of the filtered fluctuations at frequency f per Hz bandwidth.

$$S_Q = \frac{\langle(\Delta V_Q)^2\rangle}{\Delta f} = \frac{\langle(\Delta R)^2\rangle}{I^2 \Delta f} \sum_{\substack{\text{all}\\ \text{squares}}} [i_x \tilde{i}_x + i_y . \tilde{i}_y]^2 \qquad (3)$$

Now $\langle(\Delta V_Q)^2\rangle$ and $\langle(\Delta R)^2\rangle$ stands for the variance of the filtered fluctuations at frequency f in a bandwidth Δf. The simulation computer program we used provides a d.c. analysis and a first order sensitivity analysis of each network elemenet with respect to a selected pair of nodes Q. We then denote the added and squared sensitivity L_s inside on "L-shape" as

$$L_s = (i_x . \tilde{i}_x + i_y . \tilde{i}_y)/I^2 \qquad (4)$$

because, owing to the homogeneous statistical noise properties, $\langle(\Delta R)^2\rangle$ is the same for all squares in the conductor, and S_Q equals $\langle(\Delta R)^2\rangle(\Sigma L_s)/\Delta f$.

2. Spatial noise distribution

As the simulation program provides the sensitivity $\frac{\delta V_Q}{\delta R}$ of each resistor, it gives us the opportunity to study the noise distribution in the conductor. Therefore, we divided the value of L_s of each "L-form" area into four classes.

class 1: $L_s < M/5$
class 2: $L_s < M/2$
class 3: $L_s > 2*M$
class 4: $L_s > 5*M$

where M is the average value of L_s. In order to find the areas with a large or a small contribution to the noise at the sensors, we programmed the computer to plot the "L-form" areas if their representing L_s values fall in one of the classes 1 and 4. This gives a picture of the spatial noise distribution. Three examples of such pictures are given in fig. 3, fig. 4 and fig. 5. The total of the L_s values belonging to class 1 is smaller than that of class 2, and the total of the L_s values belonging to class 4 is smaller that that of class 3.

For instance, the horizontally hatched areas around the contacts D, Q in fig. 3 are together about 5 per cent of the total surface while their contribution to the total noise power S_Q is 82 per cent. The vertically hatched area, however, is about 65 per cent of the total surface and its contribution to S_Q is only 2 per cent.

When sensor and current electrodes coincide as in fig. 3, we see that, because $S_Q \propto \Sigma(i_x^2+i_y^2)^2$, areas with a high current density give the largest contribution to the total noise power. As can be seen in fig. 3, such areas are around the current carrying electrodes.

Fig. 4 shows a three probe and fig. 5 a four-probe problem. Next to these figures are denoted the percentages of the total noise contributed by each class. Fig. 5 is a good example to demonstrate that neither i nor $\tilde{i}$ is dominant for the total noise but the dot product $(i_x.\tilde{i}_x+i_y.\tilde{i}_y)$ is. At the contacts D_1, D_2 the adjoint current density is almost zero, and at Q_1, Q_2 the current density is almost zero. In the centre of the cross, i and $\tilde{i}$ are large, but $i.\tilde{i}$ is negligibly small due to the fact that i is almost perpendicular to $\tilde{i}$.

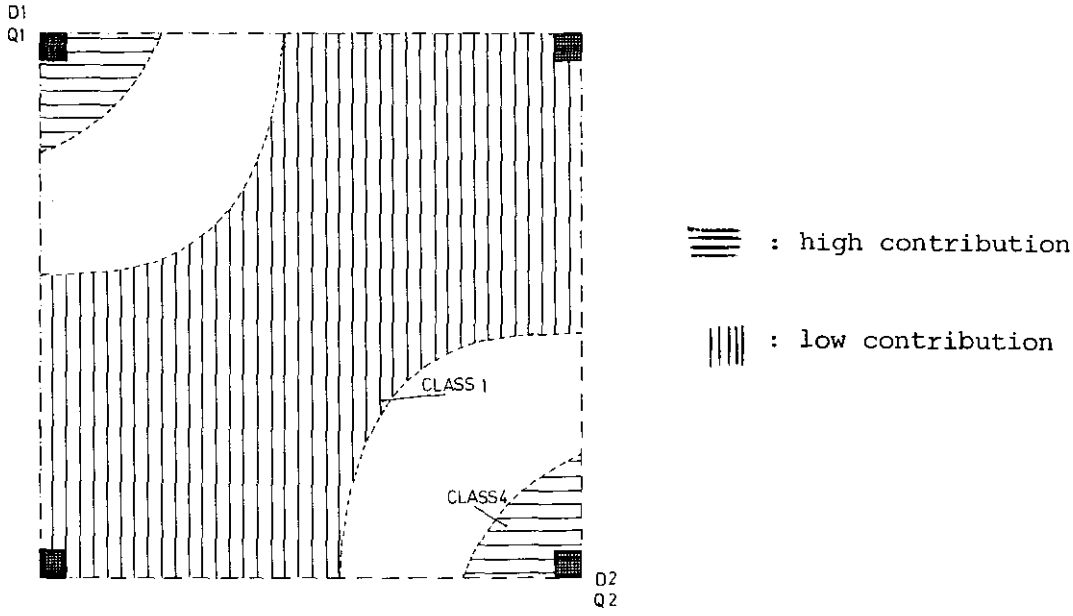

Fig. 3: Spatial noise distribution in a two-contact arrangement

	each L_s	total area contribution
class 1	< 0.2 M	2 %
class 2	< 0.5 M	5 %
class 3	> 2 M	90 %
class 4	> 5 M	82 %

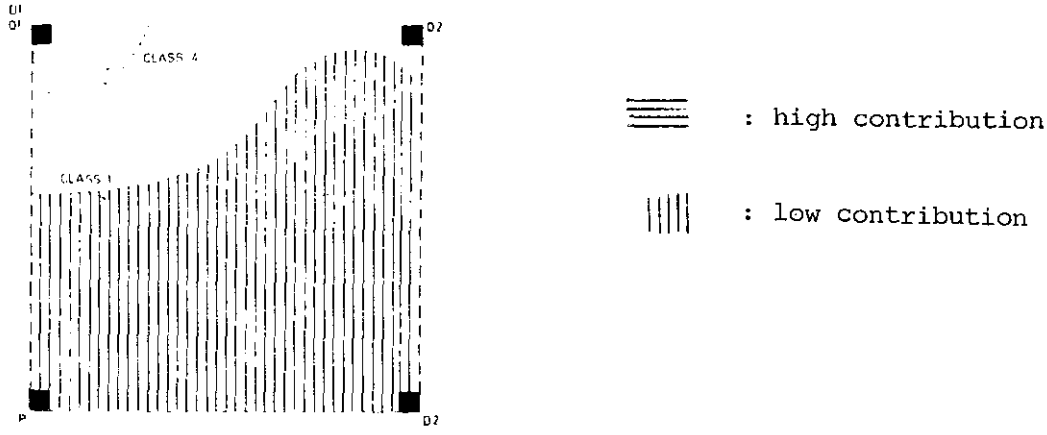

Fig. 4: Spatial noise distribution in a three-contact arrangement

	each L_s	total area contribution
class 1	< 0.2 M	2 %
class 2	< 0.5 M	3 %
class 3	> 2 M	92 %
class 4	> 5 M	87 %

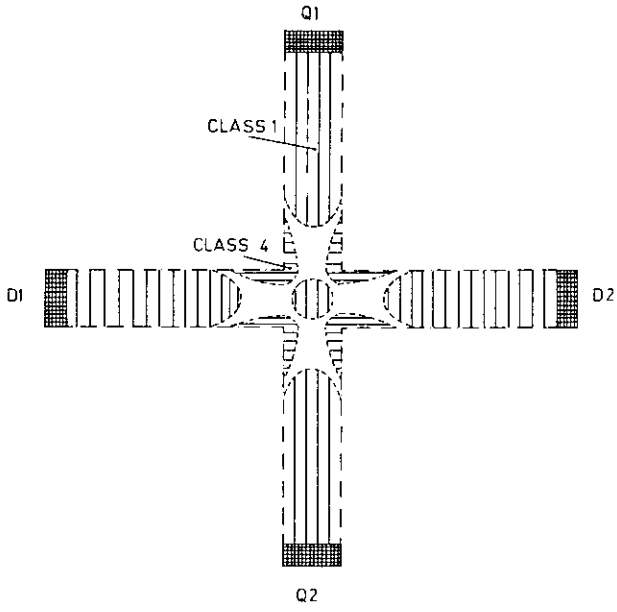

Fig. 5: Spatial noise distribution in a four-contact arrangement

	each L_s	total area contribution
class 1	< 0.2 M	0.3 %
class 2	< 0.5 M	4 %
class 3	> 2 M	96 %
class 4	> 5 M	84 %

A survey of the spatial noise distribution of 2, 3 and 4-point situations for various $2\ell/L$ ratios of the geometries in Figs.1a and 1b is given in Appendix B.

3. Comparison between experimental results and calculations

We calculated the noise power in the situations given in fig. 1 and checked some of them with 1/f noise on carbon sheet resistors. The geometry of the samples of fig. 1 was varied from $2\ell/L = 0.1$ to $2\ell/L = 0.9$. For 1/f conductivity fluctuations across a square with sheet resistance $R_\square(\Omega)$ and a surface A corresponding to the area of the "L-form" (representing a square of unit area) and submitted to a homogeneous field, we use [6]

$$\left\langle \left(\frac{\Delta R}{R_\square}\right)^2 \right\rangle = C \frac{\Delta f}{f} = \frac{C_{us}}{A} \frac{\Delta f}{f} \qquad (5)$$

where C and C_{us} are the relative 1/f noise power density at 1 Hz for the whole conductor and for a unit square respectively, Δf is the bandwidth of the

filter at frequency f. Owing to a discretisation of 20 or 18 resistors for a length L, A equals L^2/K in our computer simulation . K is the number of "L-shape" areas in a square with side L. For fig. 1a and fig. 1c K equals 340; for fig. 1b K equals 420.

Using (3), (4) and (6) we find

$$S_Q = \frac{R_{\square us}^2 C_{us}}{I^2 f A} \sum_{\substack{\text{all} \\ \text{squares}}} (i_x \tilde{i}_x + i_y \tilde{i}_y)^2 = \left(\frac{I_e}{I}\right)^2 \frac{R_{\square us}^2 C_{us}}{f} \frac{K}{L^2} \Sigma L_s \qquad (6)$$

and, in case sensor and driver electrodes coincide,

$$S_D = \frac{R_{\square us}^2 C_{us}}{I^2 f A} \sum_{\substack{\text{all} \\ \text{squares}}} (i_x^2 + i_y^2)^2 = \left(\frac{I_e}{I}\right)^2 \frac{R_{\square us}^2 C_{us}}{f} \frac{K}{L^2} \Sigma L_s \qquad (7)$$

The L_s are presented in table 1 (p.15 to 21. incl.).

We compared the calculated ratio S_Q/S_D with the experimental S_Q/S_D ratio found on carbon paper. The results of measured and calculated ratios as a function of the $2l/L$ ratio for the various four-probe situations are plotted in figs. 6 to 9. The results show good agreement.

To compare the absolute values of S we have to standardize the L_s values which have been calculated for I = 1A to experimental current I_e. Various results are presented in table 1 in Appendix A. The difference in calculated and experimental results is mainly due to anisotropy and spreading in the carbon sheet resistivity. Calculations for anisotropic conductors are discussed in chapter 4 and in tables 2 and 3 of Appendix A.

The experimentally obtained results of S_Q on a sample geometry of fig. 1 can be analyzed in terms of C_{us}. Knowing l, L, and I_e and measuring $R_\square$ and S_Q at a certain frequency f, the value of C_{us} can be calculated using eq. (6) or (7) and the calculated sum of L_s presented in table 1 in Appendix A. There the ΣL_s are presented for two- three- and four-probe arrangements on samples with a geometry given by fig. 1.

It is our experience that a sample can be considered to be two-dimensional, if the thickness δ of the film (such as the epitaxial layer or the diffused or implanted impurity layer) is below L/20. For non-granular samples, C_{us} equals α/N_I, with N_I the surface concentration (m^{-2}) of the free charge carriers in the sample, and α a dimensionless constant of the order of 10^{-3} [5].

For granular structures such as used in thick-film resistors C_{us} is dominated by the noise at the contacts between grains [6].

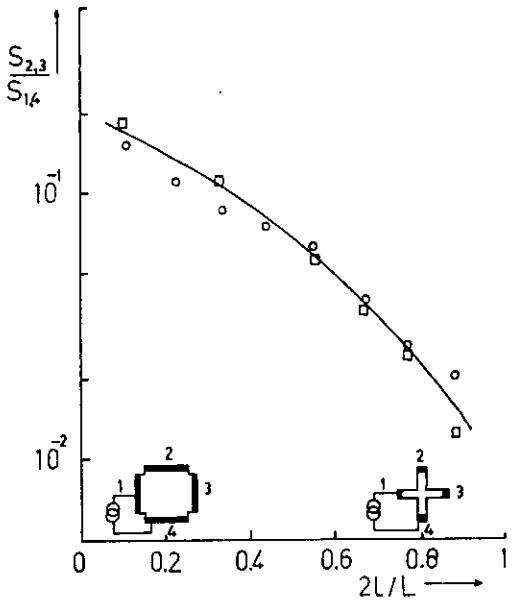

Fig. 6: S_Q/S_D ratios as a function of $2l/L$ for a cross-shaped sample with $\langle V_Q \rangle \neq 0$

□ : calculated

o : experimentally observed results

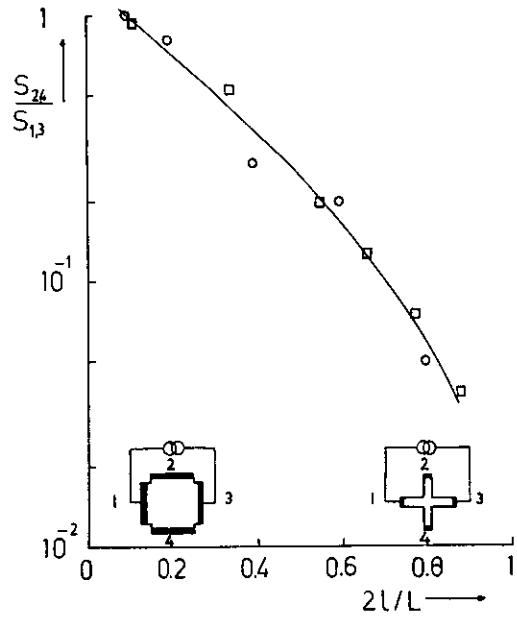

Fig. 7: S_Q/S_D ratios as a function of $2l/L$ for a cross-shaped sample with $\langle V_Q \rangle = 0$

□ : calculated results

o : experimentally observed results

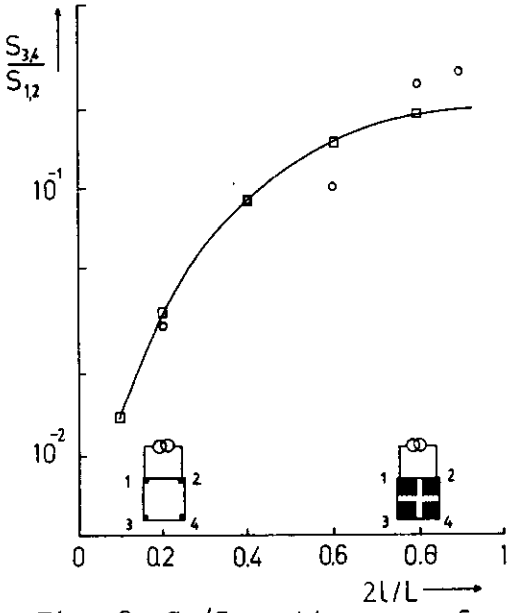

Fig. 8: S_Q/S_D ratios as a function of $2l/L$ for square-shaped samples with four corner contacts and $\langle V_Q \rangle \neq 0$

□ : calculated results

o : experimentally observed results

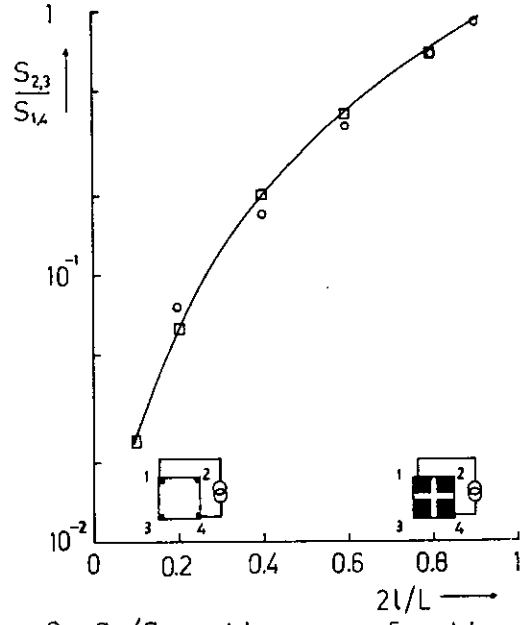

Fig. 9: S_Q/S_D ratios as a function of $2l/L$ for square-shaped samples with four corner contacts and $\langle V_Q \rangle = 0$

□: calculated results

o : experimentally observed results

4. Anisotropy

In some cases in table 1 in Appendix A there is a difference between calculated and observed S_Q values. Part of these differences is caused by an anisotropy of the carbon sheet resistor of about 25 per cent. Another part is due to some inhomogeneities in the sheet resistor characteristics such as $R_\square$ and C_{us}. To investigate this anisotropy numerically, we replaced all vertical resistors of the network by resistors of 1.25Ω instead of 1Ω. The effect was losses of symmetry.The samples no longer are invariant for rotation of 90° degrees.

Table 2 of Appendix A shows calculated results for the geometry of fig. 1b with the current source connected to contacts (1, 2) and to contacts (1, 3). If there is no anisotropy, there is no difference between the columns D_{12} and D_{13} and the results are equal to the results presented in table 1. Table 2 shows difference when the anisotropy is 25 per cent. Further we compared situations with anisotropy with their corresponding situations without anisotropy.

Table 3 of Appendix A shows the results. As can be seen, differences of factor two are possible. So the anisotropy is a reasonable explanation of differences between observed and calculated results in table 1 of Appendix A. Note that the influence of anisotropy strongly depends on terminal shape and geometry.

5. Discretisation error

If the discretisation is smaller, the number of resistors increases and the currents i and $\tilde{\imath}$ become smaller, while ΣL_s also becomes smaller. However, the ratio $(\Sigma L_s)/A$ remains about constant if the discretisation is small enough.

In order to investigate the discretisation error we modelled fig. 1c twice.

1. The total length L simulated by 12 resistors.
2. The total length L simulated by 18 resistors.

We choose fig. 1c because this is the most sensitive geometry to discretisation errors.Since the noise is inversely proportional to the "L-form" area A and proportional to L_s, the value of L_s was stadardized for the small network (larger A values) by the factor 0.466 wich is the ratio of the small to the large A values.

Fig. 10 shows the results. The difference between the dotted and solid lines gives an idea of the discretisation error. When L is simulated by 20 resistors there is almost no difference in the results compared with 18 resistors. We concluded that with respect to practical problems the simulation of L by 20 resistors is acceptable.

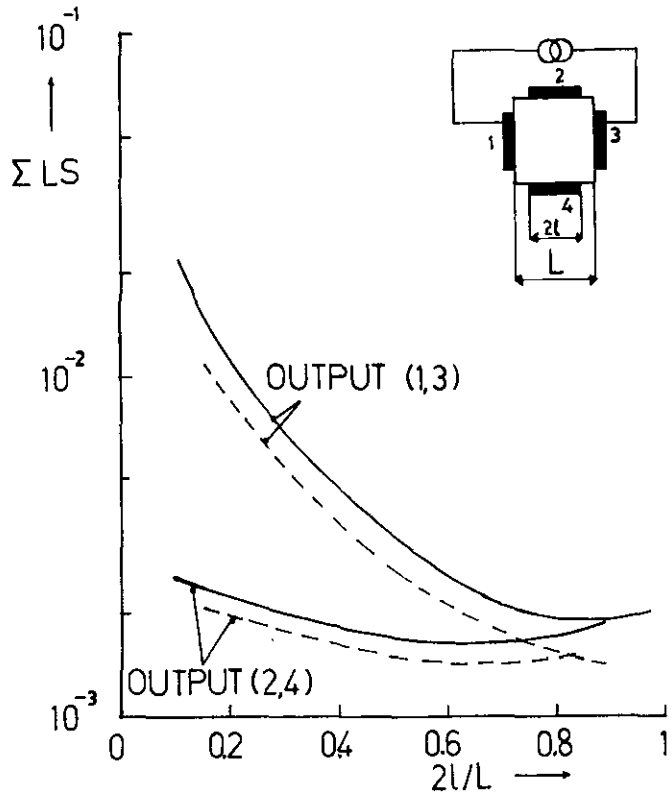

Fig. 10: The comparison $\Sigma L_s/A$ for a discretisation with 18 resistors (solid lines) and by 12 resistors (dotted line). The results are given in arbitrary units. The results with 20 resistors are about the same as with 18 resistors.

6. Discussion

Contact noise is notorious in 1/f noise investigations.
To avoid a contribution of the noise at the contacts, a sample geometry with four probes must be chosen. Among these four-probe situations, those with areas of low noise contributions around the contacts are in favour. Such a selection can be made by the aid of the spatial noise distribution charts.
If the experimentally observed ratio S_Q/S_D is much smaller than the values presented in the figures 6 to 9 for corresponding geometries, the experimental results are affected by a contact noise. This is due to the fact that in two-probe arrangements the contact noise fully contributes.
In other investigations, this method of calculation will also apply, for

instance in the calculation of the change in noise with the change of the trim cut in a thick-film resistor by using eq. (2) or eq. (5). For a two-probe arrangement the sensor and driver electrodes coincide, and $i_x = \tilde{i}_x$ and $i_y = \tilde{i}_y$ in the planar conductor. The computer program easily produces the increase in resistance and noise values with increasing trim cut.
For more complex geometries (with many edges and holes) the discretisation error arises. Choosing more "L-forms" leads to long computer process time. Therefore, we are limited in choosing the geometry and discretisation. However, for most practical geometries this method of calculation will apply.

Acknowledgements

We appreciate the work of Mr. J. Couwenberg who provided the drawings of the spatial noise distribution charts.

References

(1) L.K.J. Vandamme and W.M.G. van Bokhoven, Appl. Phys. 14, 205 (1977).

(2) W.M.G. van Bokhoven, Arch. Elektron. & Uebertragungstechn. 32, 349 (1978).

(3) S.W. Director, Circuit Theory: A Computational Approach. New York: Wiley, 1975. P. 165.

(4) P. Penfield, Jr., R. Spence and S. Duinker, Tellegen's Theorem and Electrical Networks. Cambridge, Mass.: M.I.T. Press, 1970. Research Monograph No. 58. P. 79-100.

(5) F.N. Hooge and L.K.J. Vandamme, Phys. Lett. 66A, 315 (1978).

(6) L.K.J. Vandamme, Electrocompon. Sci. & Technol. 4, 171 (1977).

(7) L.K.J. Vandamme and L.P.J. Kamp, J. Appl. Phys. 49 (1978). In press.

(8) L.J. van der Pauw, Philips Res. Rep. 13, 1 (1958).

Appendix A Numerical and experimental results

Let us first code the geometry terminal shape and $2\ell/L$ ratio using the following key consisting of 5 sets of parameters.

- A, B or C denotes the geometry of fig. 1a, 1b or 1c respectively.
- 2, 3, 4 denotes a two, three or four probe situation.
- N or O denotes whether the drivers are connected to contacts next to each other or opposite to each other.
- n or o denotes whether the sensors are connected next to each other or opposite to each other.
- 1.1,3.3,...,8.8 denoted the $2\ell/L$ ratio multiplied by 10.

So A 4 O o 6.6 denotes a cross shaped sample, considering a 4 terminal situation, with the driver contacts opposite to each other, the sensor contacts also opposite to each other and the $2\ell/L$ ratio is 0.66.
After each situation code the following information is denoted in six columns

- ΣL_s : This column denotes the sum of the added and squared sensitivities in all L-shapes according to the sum in the R.H.S. of eq. (3) or eq. (4).

- V_Q : Denotes the d.c. voltage between the sensor electrodes when a current of 1A is passed through the driver electrodes and the sheet resistance is 1Ω. For four-probe arrangements, when the driver and sensor electrodes are next to each other and the contact length is small in comparison with the hole length of the boundary of the sheet, we can expect $V_Q \approx \frac{\ln 2}{\pi} = 0.22$ following van der Pauw's result [7]. Using the following expression

$$R_\square = \frac{V_e}{I_e} \cdot \lambda(2\ell/L)$$

we can calculate the sheet tesistivity. In the calculations $R_\square = 1\Omega$ and $I = 1A$, so $(2\ell/L)$ equals $1/V_Q$ obtained from table 1. Measuring V_e and I_e, we can calculate the sheet resistance $R_\square$ of any sample with the same geometry.

- percentages : This column denotes the contribution per cent of the classes 1 to 4 incl. in this sequence with respect to the total given in the first column.
When the percentages of all classes are low, it means that the noise is homogeneously distributed. The percentages for geometry C have not been calculated. Owing to the accuracy of the calculation all percentages are rounded off to integers.

- calculated S_Q : If there is a corresponding experimental result (same geometry in the next column, this column gives the calculated S_Q using eq. (6) and the following data:

All situations:
- $f = 1$ Hz
- $I_{cal} = 1$ Amp.
- $R_Q = 4k5$
- $C_{us} = 5 \times 10^{-10}$ (cm^2).

A4 and A3 situations:
- $I_e = 90$ µA
- $L = 10.4$ cm
- Number of "L-form" areas $K = 340$
- $A = 0.32$ cm^2

A_2 situations:
- $I_e = 55$ µA
- $L = 13.6$ cm
- Number of "L-form" areas $K = 340$
- $A = 0.54$ cm^2

B situations:
- $I_e = 55$ µA
- $L = 15$ cm
- Number of "L-form"areas $K = 340$
- $A = 0.54$ cm^2

C situations:
- $I_e = 90$ µA
- $L = 12$ cm
- Number of "L-form" areas $K = 340$
- $A = 0.42$ cm^2

- experimental S_Q : The experimentally observed results of S_Q measured under conditions as described in the foregoing column.

- spatial distribution chart on page : This column gives the number of the page where a chart of the spatial noise distribution of this situation is shown.

TABLE 1

Situation code	ΣL_s	V_Q (V)	Percentages	Cal. S_Q	Exp. S_Q	Distr. Plot Page:
A4 Oo 1.1	3.2×10^{-3}	0	1,3,90,90	8.2×10^{-13}	2.0×10^{-12}	25
A4 Oo 3.3	2.6×10^{-3}	0	2,5,83,57	6.8×10^{-13}	1.8×10^{-12}	25
A4 Oo 5.5	3.5×10^{-3}	0	2,5,70,52	9.1×10^{-13}	4.5×10^{-12}	26
A4 Oo 6.6	5.0×10^{-3}	0	2,6,81,64	1.3×10^{-12}	3.5×10^{-12}	26
A4 Oo 7.7	9.1×10^{-3}	0	2,5,84,78	2.4×10^{-12}	8.1×10^{-12}	27
A4 Oo 8.8	2.2×10^{-2}	0	0,4,96,84	5.7×10^{-12}	4.0×10^{-11}	27
A4 Nn 1.1	9.0×10^{-4}	0.12	2,3,94,87	2.3×10^{-13}	5.9×10^{-13}	28
A4 Nn 3.3	7.2×10^{-4}	0.18	3,9,80,63	1.9×10^{-13}	5.2×10^{-13}	28
A4 Nn 5.5	1.1×10^{-3}	0.21	2,7,60,43	2.9×10^{-13}	1.2×10^{-12}	29
A4 Nn 6.6	1.6×10^{-3}	0.22	2,7,63,45	4.2×10^{-13}	1.2×10^{-12}	29
A4 Nn 7.7	3.0×10^{-3}	0.22	1,5,81,49	7.8×10^{-13}	2.3×10^{-12}	30
A4 Nn 8.8	7.5×10^{-3}	0.22	1,2,85,62	1.9×10^{-12}	1.2×10^{-11}	30
A3 Nn 1.1	1.4×10^{-3}	0.15	2,4,92,86	3.6×10^{-13}	1.1×10^{-12}	31
A3 Nn 3.3	2.3×10^{-3}	0.52	3,5,87,65	6.0×10^{-13}	1.1×10^{-12}	31
A3 Nn 5.5	8.3×10^{-3}	0.65	3,4,92,82	2.2×10^{-12}	3.7×10^{-12}	32
A3 Nn 6.6	2.0×10^{-2}	0.94	2,3,92,86	5.2×10^{-12}	7.0×10^{-12}	32
A3 Nn 7.7	5.9×10^{-2}	1.47	1,2,96,89	1.5×10^{-11}	2.6×10^{-11}	33
A3 Nn 8.8	3.0×10^{-1}	2.70	1,1,98,95	7.8×10^{-11}	1.6×10^{-10}	33
A3 No 1.1	2.7×10^{-3}	0.26	2,4,92,86	7.0×10^{-13}	1.6×10^{-12}	34
A3 No 3.3	3.3×10^{-3}	0.52	2,5,83,61	8.6×10^{-13}	1.5×10^{-12}	34
A3 No 5.5	9.8×10^{-3}	0.87	2,5,87,72	2.6×10^{-12}	3.5×10^{-12}	35
A3 No 6.6	2.2×10^{-2}	1.16	2,3,92,83	5.6×10^{-12}	7.5×10^{-12}	35
A3 No 7.7	6.3×10^{-2}	1.68	1,2,93,89	1.6×10^{-11}	2.6×10^{-11}	36
A3 No 8.8	3.1×10^{-1}	2.91	0,1,96,90	8.1×10^{-11}	1.8×10^{-10}	36

TABLE 1 (continued)

Situation code	ΣL_s	V_Q (V)	Percentages	Cal. S_Q	Exp. S_Q	Distr. Plot Page:
A2 Nn 1.1	5.1×10^{-3}	0.42	2,3,95,91	2.9×10^{-13}	6.0×10^{-13}	37
A2 Nn 3.3	6.3×10^{-3}	0.86	2,4,83,70	3.6×10^{-13}	1.1×10^{-12}	37
A2 Nn 5.5	1.9×10^{-2}	1.52	1,2,89,51	1.1×10^{-12}	2.9×10^{-12}	38
A2 Nn 6.6	4.3×10^{-2}	2.10	1,2,92,36	2.5×10^{-12}		38
A2 Nn 7.7	1.3×10^{-1}	3.15	1,1,93,21	7.4×10^{-12}	4.5×10^{-11}	39
A2 Nn 8.8	6.2×10^{-1}	5.60	0,1,97,10	3.6×10^{-11}		39
A2 Oo 1.1	3.3×10^{-3}	0.53	3,6,87,85	1.8×10^{-13}	4.2×10^{-13}	40
A2 Oo 3.3	4.9×10^{-3}	1.04	1,4,74,44	2.8×10^{-13}	1.1×10^{-12}	40
A2 Oo 5.5	1.7×10^{-2}	1.73	1,2,82,13	9.7×10^{-13}	2.4×10^{-12}	41
A2 Oo 6.6	4.1×10^{-2}	2.32	1,1,87, 8	2.3×10^{-12}		41
A2 Oo 7.7	1.2×10^{-1}	3.37	0,1,92, 8	6.8×10^{-12}	4.2×10^{-11}	not presented
A2 Oo 8.8	6.2×10^{-1}	5.81	0,0,96, 0	3.5×10^{-11}		42
B4 Oo 1	1.6×10^{-3}	0	1,2,85,16	9.1×10^{-14}		43
B4 Oo 2	1.6×10^{-3}	0	1,2,85, 0	9.1×10^{-14}	1.5×10^{-13}	43
B4 Oo 4	1.6×10^{-3}	0	1,2,86, 0	9.1×10^{-14}	1.9×10^{-13}	44
B4 Oo 6	1.4×10^{-3}	0	0,2,86, 0	8.0×10^{-14}	2.0×10^{-13}	44
B4 Oo 8	7.8×10^{-4}	0	0,1,80, 0	4.5×10^{-14}	8.5×10^{-14}	45
B4 Nn 1	8.6×10^{-4}	0.22	1,4, 0, 0	4.9×10^{-14}		46
B4 Nn 2	8.4×10^{-4}	0.22	1,4, 0, 0	4.8×10^{-14}	1.0×10^{-13}	46
B4 Nn 4	7.3×10^{-4}	0.20	1,3, 0, 0	4.2×10^{-14}	9.0×10^{-14}	47
B4 Nn 6	5.2×10^{-4}	0.16	1,5, 2, 0	3.0×10^{-14}	5.2×10^{-14}	47
B4 Nn 8	2.7×10^{-4}	0.09	1,1,14, 0	1.5×10^{-14}	4.0×10^{-14}	48

TABLE 1 (continued)

Situation Code	ΣL_s	V_Q (V)	Percentages	Cal. S_Q	Exp. S_Q	Distr. Plot page:
B3 Nn 1	2.8×10^{-2}	1.16	2,3,91,85	1.6×10^{-12}		49
B3 Nn 2	1.1×10^{-2}	0.85	2,4,88,78	6.3×10^{-13}	2.2×10^{-12}	49
B3 Nn 4	3.1×10^{-3}	0.48	2,5,79,57	1.8×10^{-13}	4.5×10^{-13}	50
B3 Nn 6	1.2×10^{-3}	0.26	4,6,68,31	6.8×10^{-14}	1.1×10^{-13}	50
B3 Nn 8	3.7×10^{-4}	0.11	6,7,33,15	2.1×10^{-14}	4.5×10^{-14}	51
B3 On 1	2.9×10^{-2}	1.37	3,5,90,85	1.7×10^{-12}		52
B3 On 2	1.2×10^{-2}	1.06	3,6,84,76	6.8×10^{-13}	1.5×10^{-12}	52
B3 On 4	4.1×10^{-3}	0.68	3,8,79,57	2.3×10^{-13}	7.5×10^{-13}	53
B3 On 6	1.9×10^{-3}	0.42	1,8,75,49	1.1×10^{-13}	2.0×10^{-13}	53
B3 On 8	7.6×10^{-4}	0.20	0,7,74,55	4.3×10^{-14}	9.5×10^{-14}	54
B2 Oo 1	5.7×10^{-2}	2.74	3,5,89,81	3.3×10^{-12}		55
B2 Oo 2	2.2×10^{-2}	2.12	4,8,84,71	1.3×10^{-12}	2.0×10^{-12}	55
B2 Oo 4	6.5×10^{-3}	1.37	3,9,74,47	3.7×10^{-13}	1.1×10^{-12}	56
B2 Oo 6	2.8×10^{-3}	0.84	1,6,58,28	1.6×10^{-13}	3.8×10^{-13}	56
B2 Oo 7	1.8×10^{-3}	0.61	1,3,42,23	1.0×10^{-13}		not presented
B2 Oo 8	1.1×10^{-3}	0.40	0,2,27,15	6.3×10^{-14}	1.3×10^{-13}	57
B2 Nn 1	5.9×10^{-2}	2.52	2,5,85,73	3.4×10^{-12}		58
B2 Nn 2	2.4×10^{-2}	1.90	1,4,79,61	1.4×10^{-12}	3.2×10^{-12}	58
B2 Nn 4	8.0×10^{-3}	1.16	2,5,80,41	4.6×10^{-13}	1.0×10^{-12}	59
B2 Nn 6	3.6×10^{-3}	0.68	4,6,86,23	2.1×10^{-13}	5.0×10^{-13}	59
B2 Nn 8	1.4×10^{-3}	0.31	3,4,94, 8	8.0×10^{-14}	1.6×10^{-13}	60

TABLE 1 (continued)

Situation code	ΣL_s	V_Q (V)	Cal. S_Q	Exp. S_Q
C4 Oo 1.1	2.5×10^{-3}	0 V	5×10^{-13}	3.4×10^{-12}
C4 Oo 2.2	2.3×10^{-3}	0 V	4.6×10^{-13}	2.8×10^{-12}
C4 Oo 3.3	2.2×10^{-3}	0 V	4.4×10^{-13}	3.5×10^{-12}
C4 Oo 6.6	1.7×10^{-3}	0 V	3.4×10^{-13}	2.0×10^{-12}
C4 Oo 8.8	1.9×10^{-3}	0 V	3.8×10^{-13}	2.2×10^{-12}
C4 Nn 1.1	7.4×10^{-4}	0.22	1.5×10^{-13}	9.2×10^{-13}
C4 Nn 2.2	6.6×10^{-4}	0.21	1.3×10^{-13}	8.0×10^{-13}
C4 Nn 3.3	6.3×10^{-4}	0.20	1.3×10^{-13}	8.0×10^{-13}
C4 Nn 6.6	4.9×10^{-4}	0.15	9.8×10^{-14}	5.5×10^{-13}
C4 Nn 8.8	6.0×10^{-4}	0.10	1.2×10^{-13}	7.4×10^{-13}
C3 Nn 1.1	1.1×10^{-2}	0.63	2.2×10^{-12}	2.9×10^{-11}
C3 Nn 2.2	5.2×10^{-3}	0.50	1.0×10^{-12}	5.3×10^{-12}
C3 Nn 3.3	3.0×10^{-3}	0.40	6.0×10^{-13}	2.8×10^{-12}
C3 Nn 6.6	1.0×10^{-3}	0.22	2.0×10^{-13}	9.0×10^{-13}
C3 Nn 8.8	9.0×10^{-4}	0.12	1.8×10^{-13}	1.0×10^{-12}
C3 No 1.1	1.3×10^{-2}	0.85	2.6×10^{-12}	3.1×10^{-11}
C3 No 2.2	6.2×10^{-3}	0.70	1.2×10^{-12}	5.7×10^{-12}
C3 No 3.3	3.9×10^{-3}	0.60	7.8×10^{-12}	3.8×10^{-12}
C3 No 6.6	1.7×10^{-3}	0.37	3.4×10^{-13}	1.4×10^{-12}
C3 No 8.8	1.7×10^{-3}	0.21	3.4×10^{-13}	2.4×10^{-12}
C2 Oo 1.1	2.2×10^{-2}	1.70	4.4×10^{-12}	1.9×10^{-10}
C2 Oo 2.2	1.1×10^{-2}	1.41	2.2×10^{-12}	3.2×10^{-11}
C2 Oo 3.3	6.5×10^{-3}	1.20	1.3×10^{-12}	2.6×10^{-11}
C2 Oo 6.6	2.3×10^{-3}	0.73	4.6×10^{-13}	4.1×10^{-12}
C2 Oo 8.8	2.0×10^{-3}	0.43	4.0×10^{-13}	3.8×10^{-12}
C2 Nn 1.1	2.5×10^{-2}	1.50	5.0×10^{-12}	1.3×10^{-10}
C2 Nn 2.2	1.2×10^{-2}	1.20	2.4×10^{-12}	2.6×10^{-11}
C2 Nn 3.3	7.5×10^{-3}	1.00	1.5×10^{-12}	1.8×10^{-11}
C2 Nn 6.6	3.3×10^{-3}	0.58	6.6×10^{-13}	4.0×10^{-12}
C2 Nn 8.8	3.3×10^{-3}	0.33	6.6×10^{-13}	6.4×10^{-12}

TABLE 2

Situation	D_{12}		D_{13}	
	ΣL_s	V_Q	ΣLS	V_Q
B4 Nn 1	6.8×10^{-4}	0.18	1.9×10^{-3}	0.34
B4 Nn 2	6.6×10^{-4}	0.18	1.8×10^{-3}	0.34
B3 Nn 1	4.6×10^{-2}	1.28	4.6×10^{-2}	1.28
B3 Nn 2	1.2×10^{-2}	0.93	1.2×10^{-2}	0.93
B3 On 1	4.7×10^{-2}	1.45	4.7×10^{-2}	1.62
B3 On 2	1.3×10^{-2}	1.11	1.3×10^{-2}	1.27
B2 Nn 1	9.7×10^{-2}	2.73	9.8×10^{-2}	2.90
B2 Nn 2	2.7×10^{-2}	2.04	3.0×10^{-2}	2.21

Table 2: Columns denoted by D_{12} give ΣL_s and the corresponding d.c. voltage V_Q when the current source is connected to (1, 2). Column denoted by D_{13} given ΣL_s and V_Q but now with the current source is connected to (1, 3). See the figure below. The sample of fig. 1b is simulated by a resistor network with all row resistors having a value of 1.25Ω . So table 2 shows the effect of loss of symmetry. Note that in the special case of B3 Nn there is no difference in the results because in that situation we are applying the reciprocity principle and the reciprocity principle holds for this simple linear passive network.

The arrow in the fig. indicates the "easy direction" of the resistivity. In the direction perpendicular to the arrow the sheet resistance and C_{us} is 25% higher than in the arrow direction.

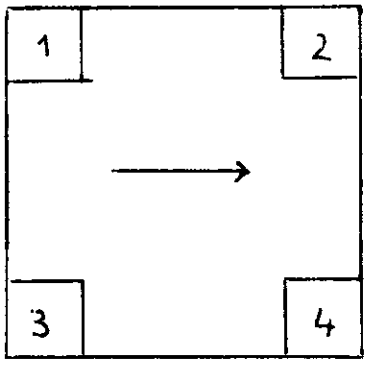

TABLE 3

Situation code	isotropic		anisotropic	
	ΣL_s	V_Q	ΣL_s	V_Q
B4 Oo 1	1.6×10^{-3}	0	2.4×10^{-3}	0.17
B4 Oo 2	1.6×10^{-3}	0	2.4×10^{-3}	0.16
B4 Nn 1	8.6×10^{-4}	0.22	6.8×10^{-4}	0.18
B4 Nn 2	8.4×10^{-4}	0.22	6.6×10^{-4}	0.18
B3 Nn 1	2.8×10^{-2}	1.16	4.6×10^{-2}	1.28
B3 Nn 2	1.1×10^{-2}	0.85	1.2×10^{-2}	0.93
B3 On 1	2.9×10^{-2}	1.37	4.7×10^{-2}	1.45
B3 On 2	1.2×10^{-2}	1.06	1.3×10^{-2}	1.11
B2 Oo 1	5.7×10^{-2}	2.74	8.8×10^{-2}	3.08
B2 Oo 2	2.2×10^{-2}		3.6×10^{-2}	2.38
B2 Nn 1	5.9×10^{-2}	2.52	9.7×10^{-2}	2.73
B2 Nn 2	2.4×10^{-2}	1.90	2.7×10^{-2}	2.04

Table 3: Columns denoted "isotropic" give ΣL_s of output Q_1, Q_2 (the ΣL_s column in table 1) and the corresponding d.c. voltage V_Q when the planar resistor of fig. 1b, is simulated by a network with all resistors having the same value. The columns denoted "anisotropic" give corresponding results when the vertical resistors are 1.25 Ω and the horizontal resistors are 1 Ω. The isotropic and anisotropic results deal with exactly the same situations, which means that not only the configuration is the same but also the terminals D and Q are connected to contacts with the same numbers.

Appendix B Spatial noise distribution

This appendix contains charts of all spatial noise distributions of the A and B situations given in Appendix A, table 1.
In the plots the conductor boundaries are represented by dotted lines. Areas with a low and high noise contribution are bordered by solid lines. When such an area is indicated by the letter "L" for low contribution, it means that all squares of unit "L-form" areas inside that area fall in class 1; when indicated by "H" for high contribution, the unit areas bordered by the solid line fall in class 4. For the exact information of each plot see Appendix A, table 1.
In all plots D_1 and D_2 are the driver electrodes, Q_1 and Q_2 the sensor electrodes.

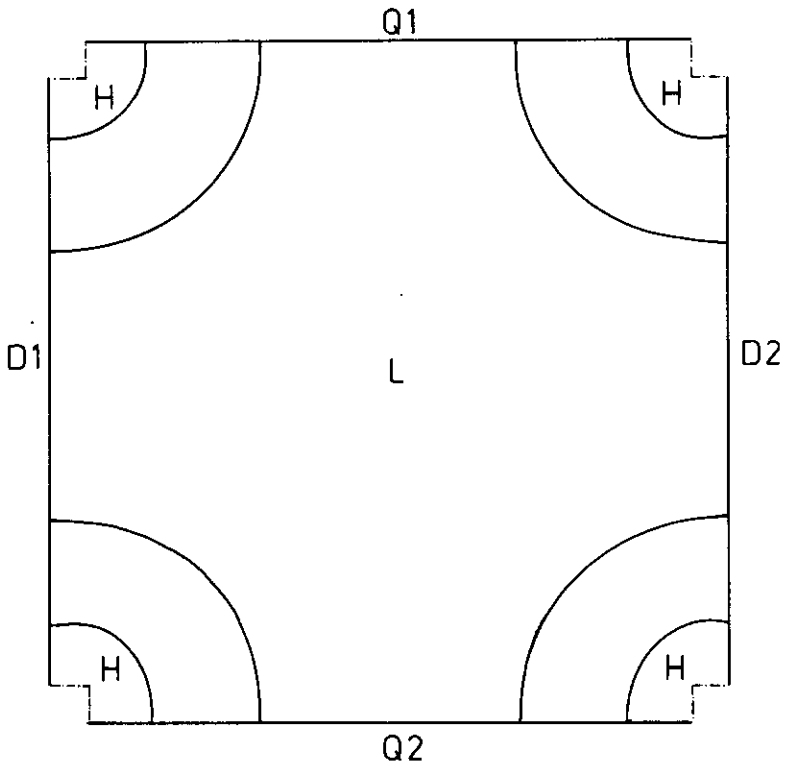
Q1
H
H
D1
L
D2
H
H
Q2

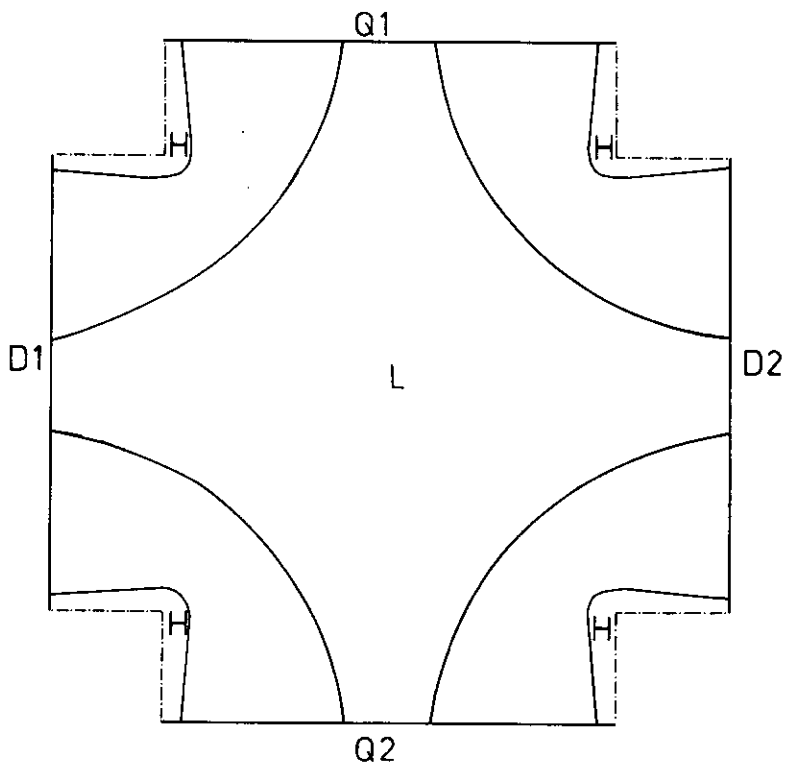
Q1
H
H
D1
L
D2
H
H
Q2

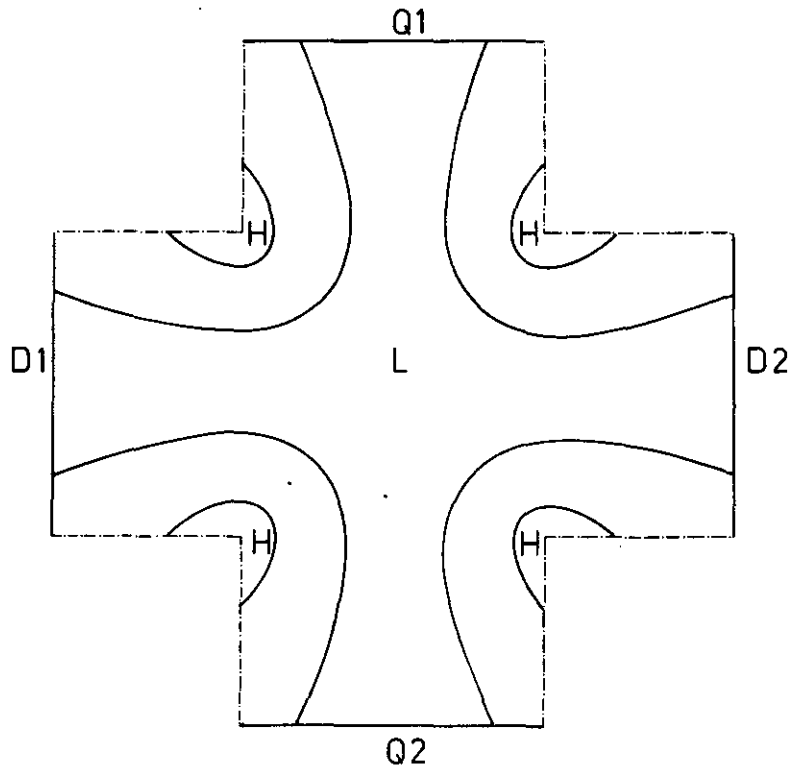
Q1
H
H
D1
L
D2
H
H
Q2

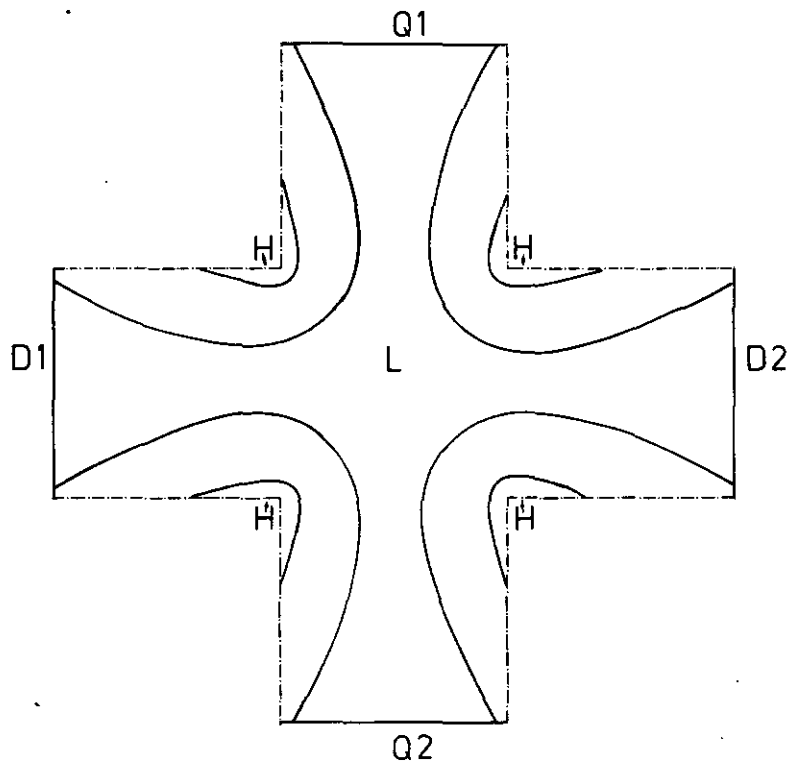
Q1
H
H
D1
L
D2
H
H
Q2

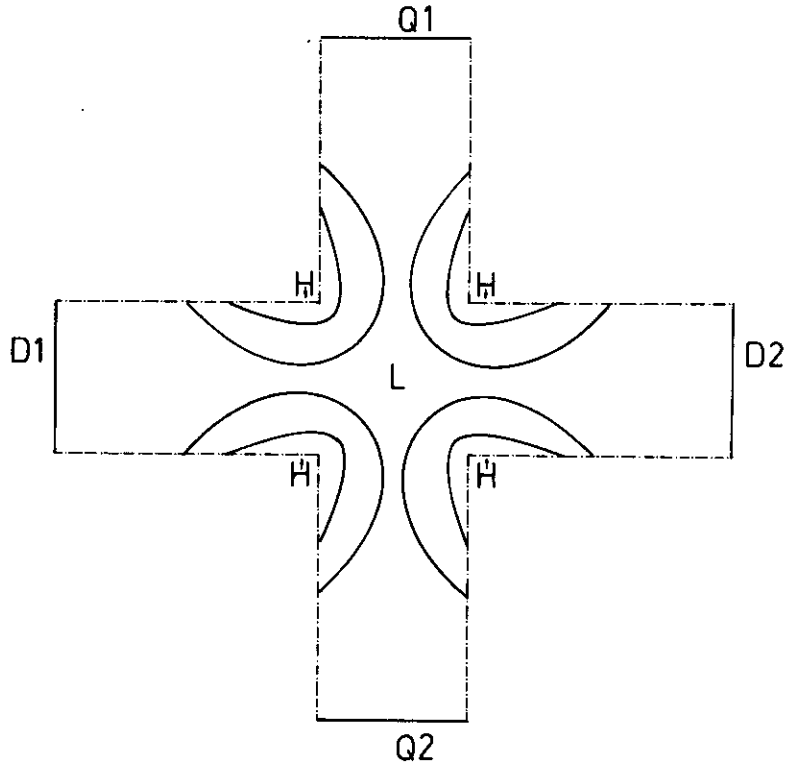
Q1
H
H
D1
L
D2
H
H
Q2

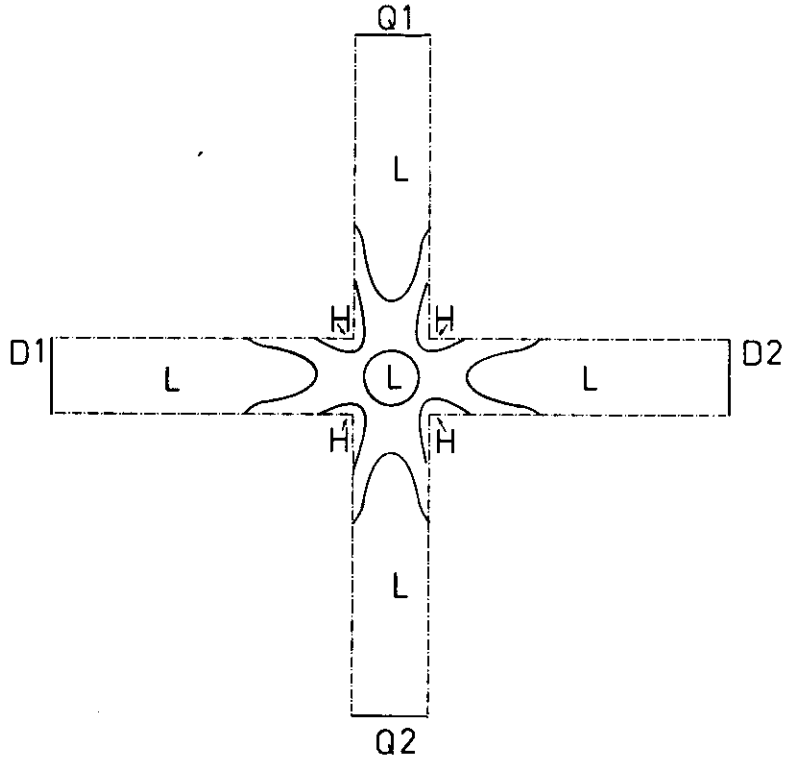
Q1
L
H
H
D1
L
L
D2
H
H
L
Q2

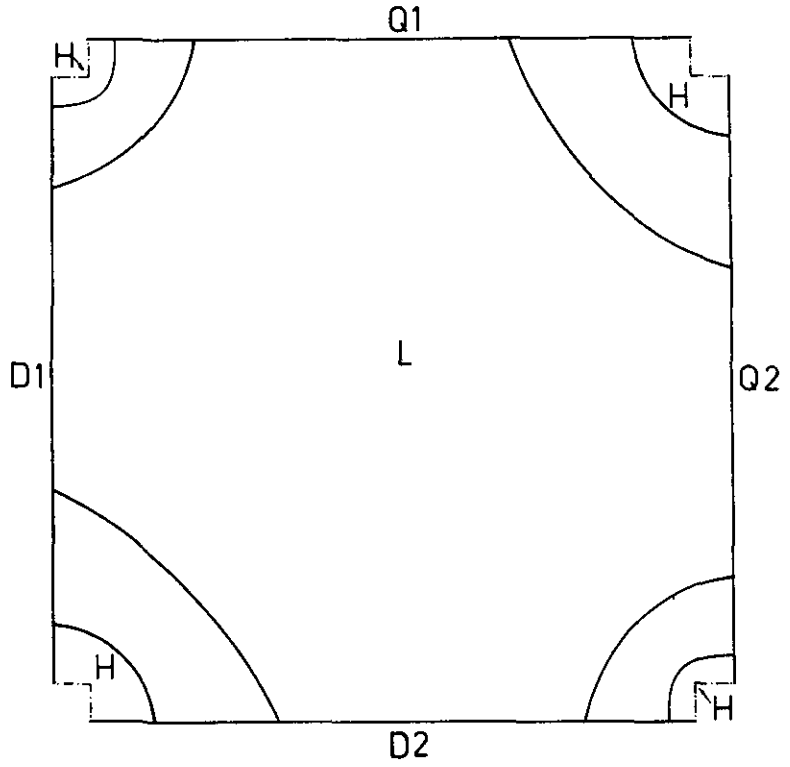
Q1
H
H
D1
L
Q2
H
H
D2

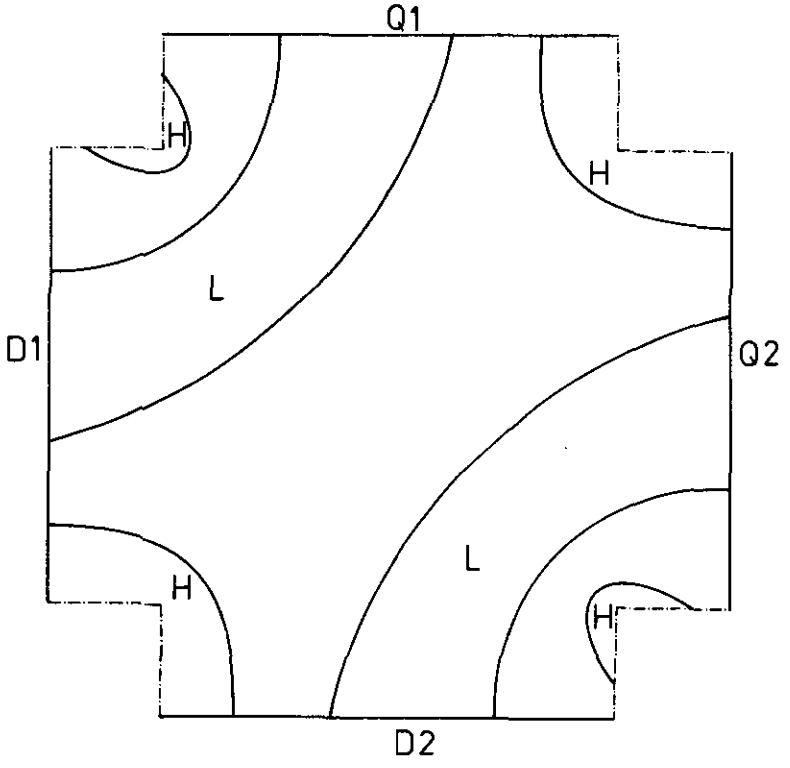
Q1
H
H
L
D1
Q2
L
H
H
D2

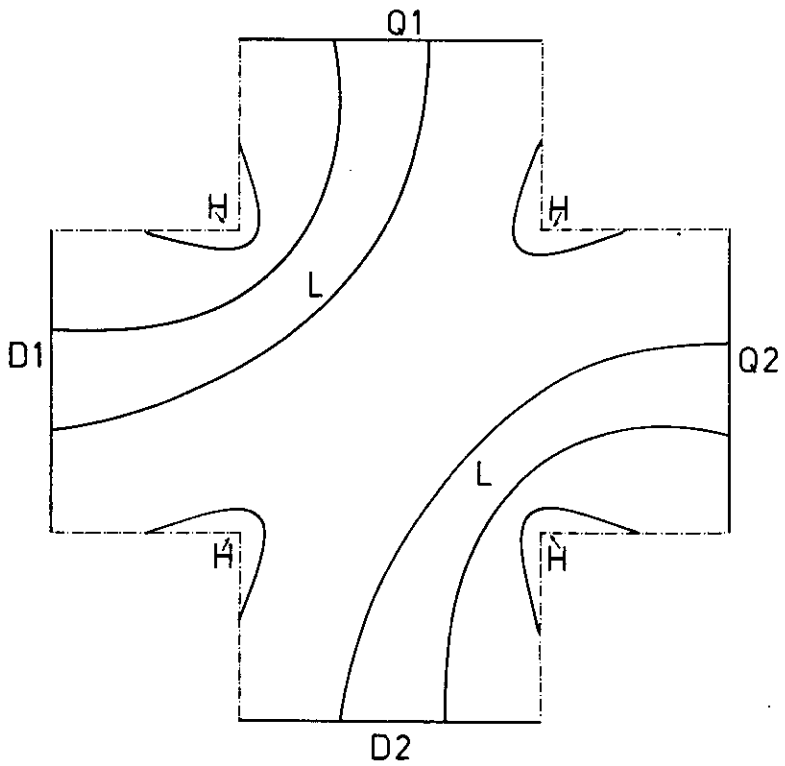
Q1
H
H
L
D1
Q2
L
H
H
D2

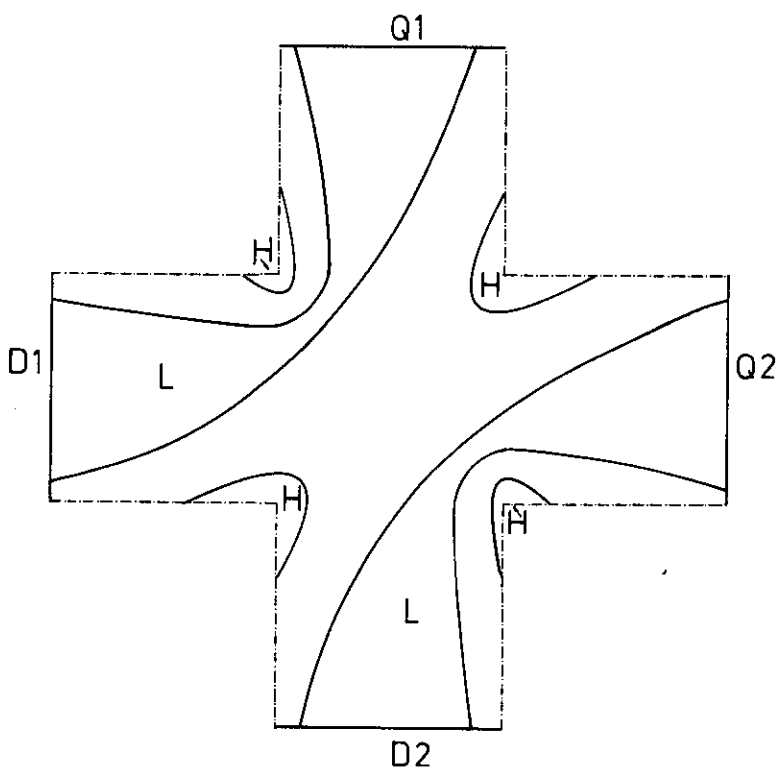
Q1
H
H
D1
L
Q2
H
H
L
D2

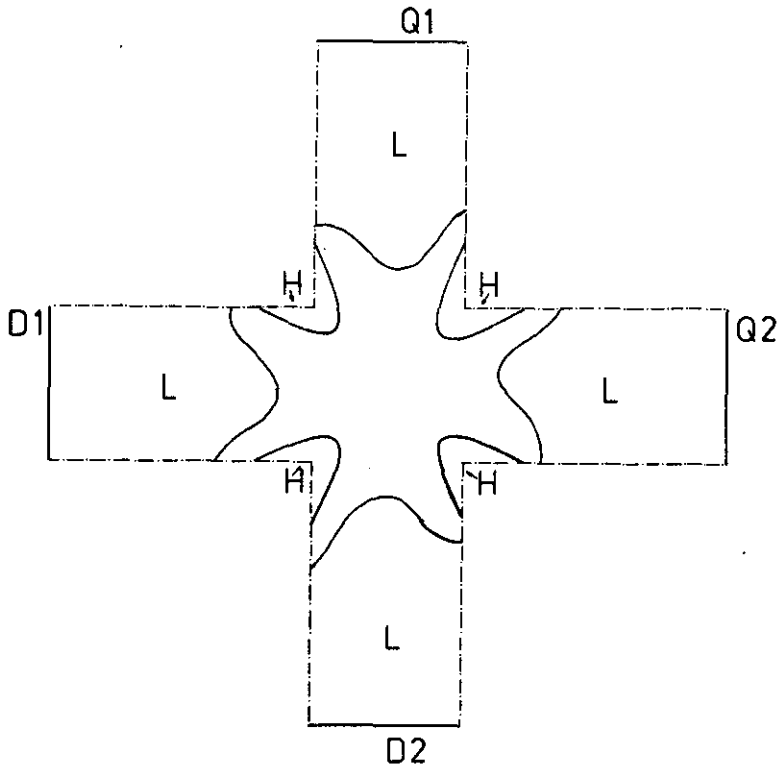
Q1
L
H
H
D1
L
L
Q2
H
H
L
D2

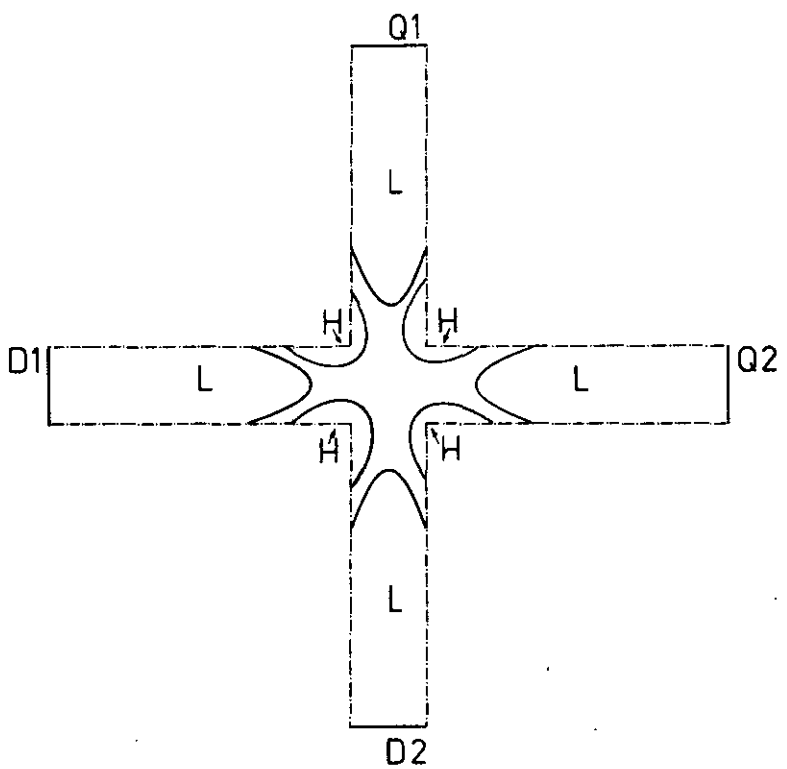
Q1
L
H
H
D1
L
L
Q2
H
H
L
D2

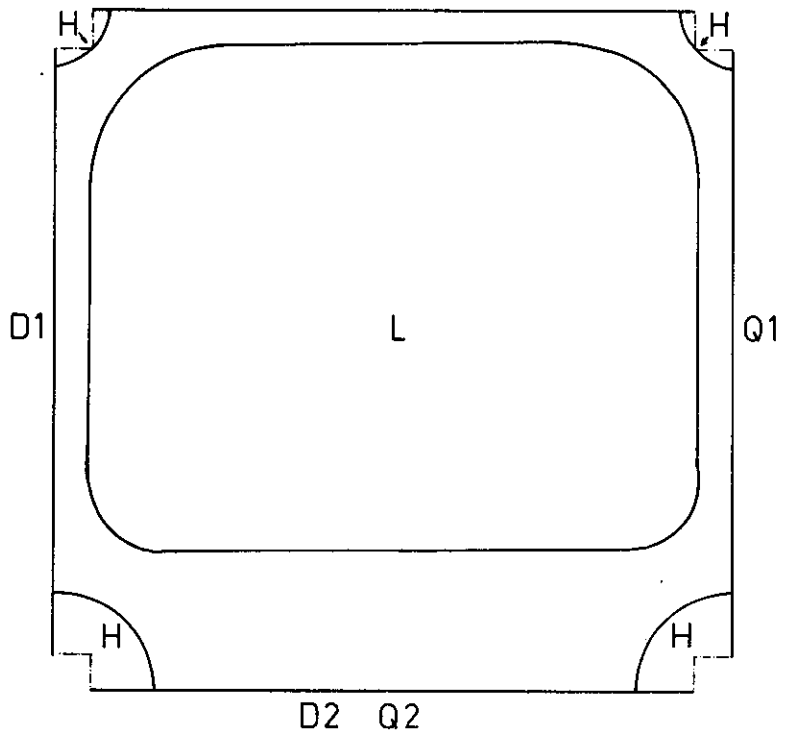
H
H
D1
L
Q1
H
H
D2
Q2

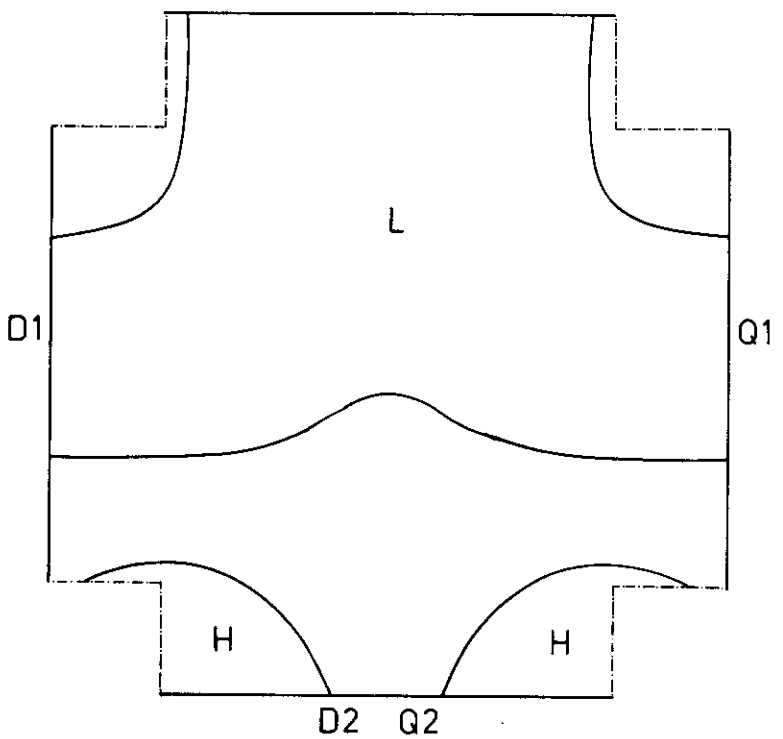
L
D1
Q1
H
H
D2
Q2

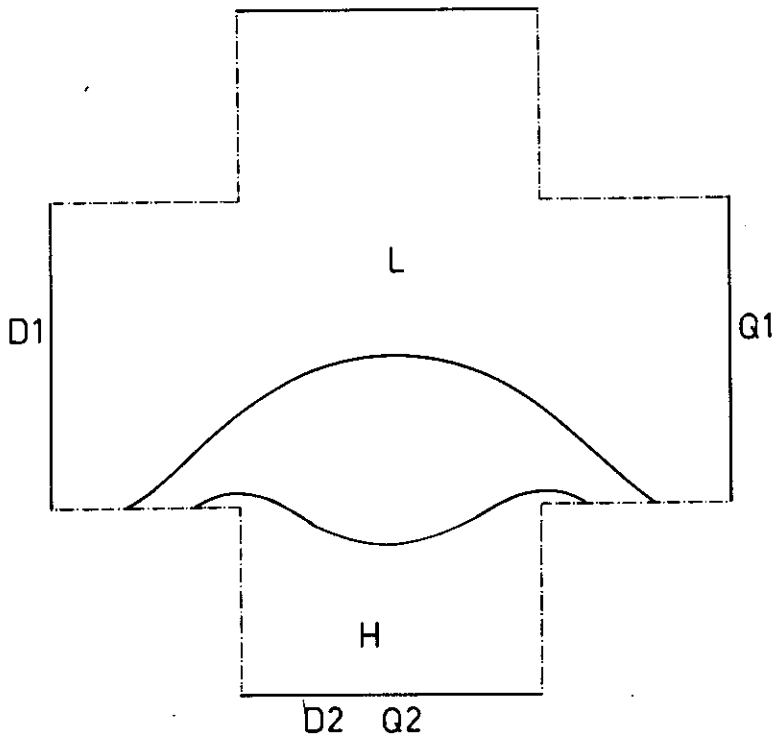
L
D1
Q1
H
D2
Q2

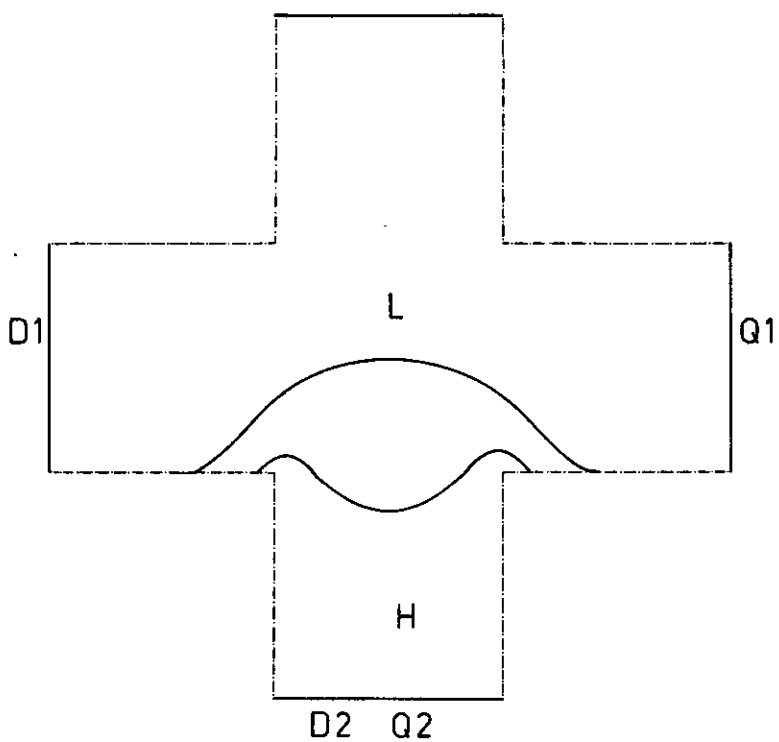
L
D1
Q1
H
D2
Q2

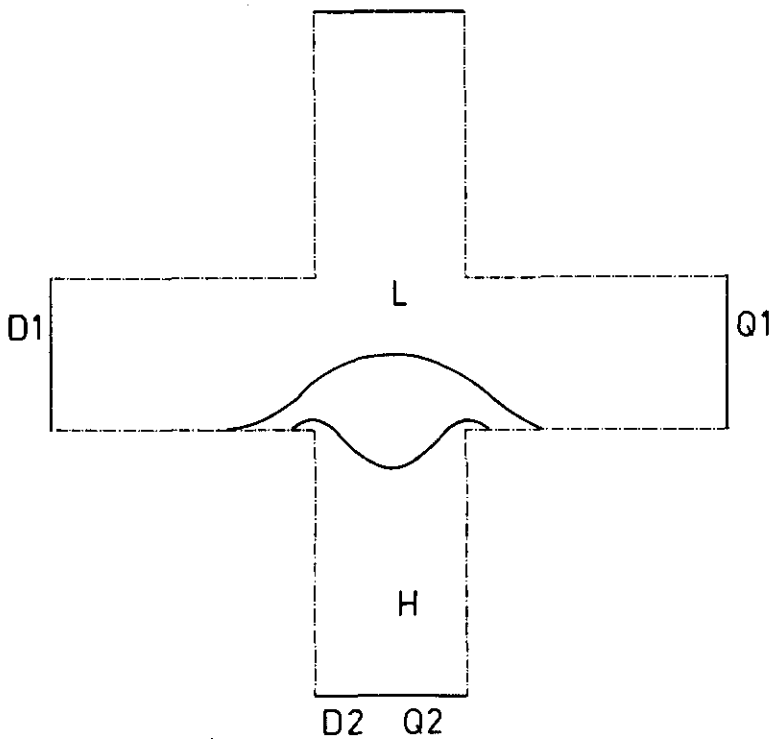
L
D1
Q1
H
D2
Q2

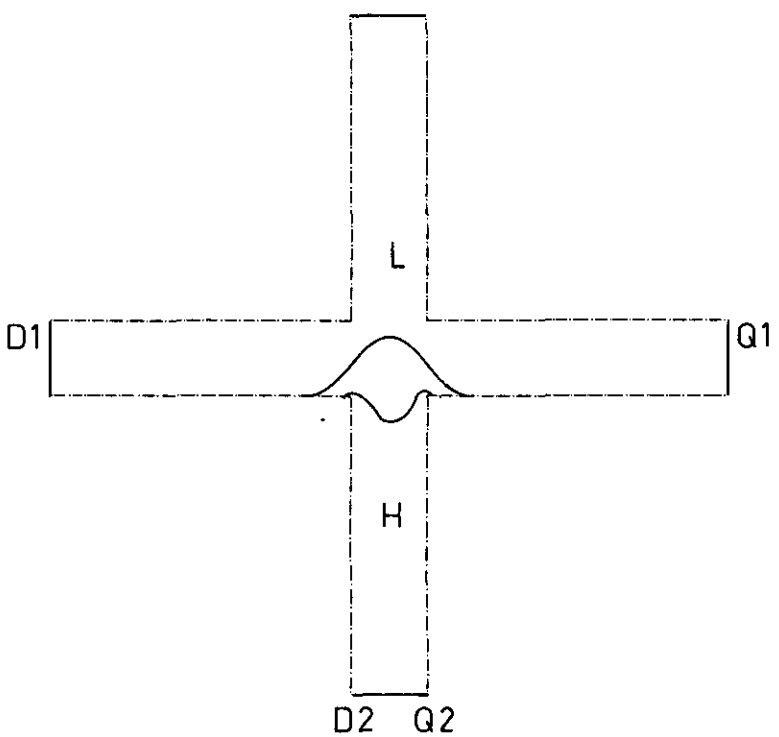
L
D1
Q1
H
D2
Q2

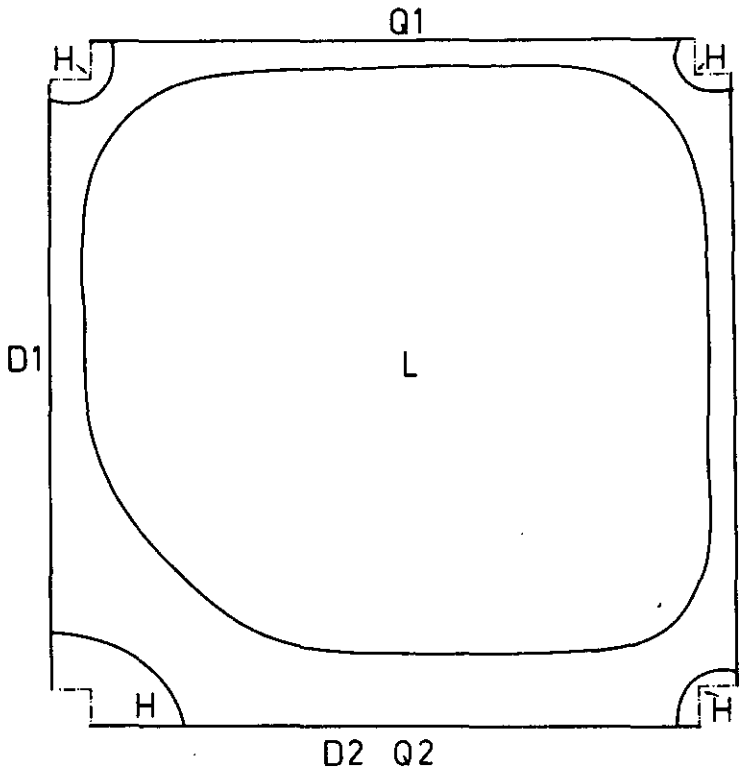
Q1
H
H
D1
L
H
H
D2 Q2

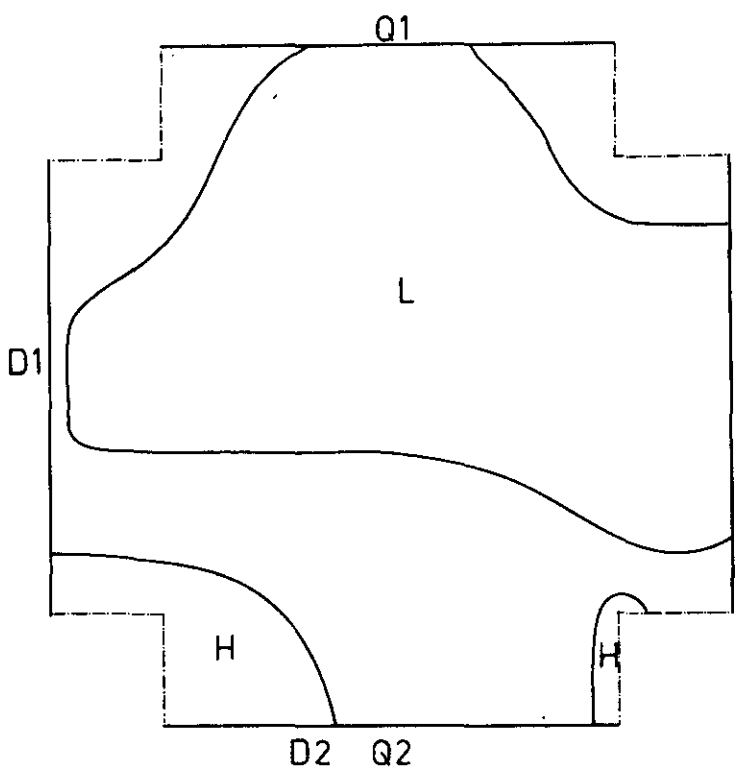
Q1
L
D1
H
H
D2 Q2

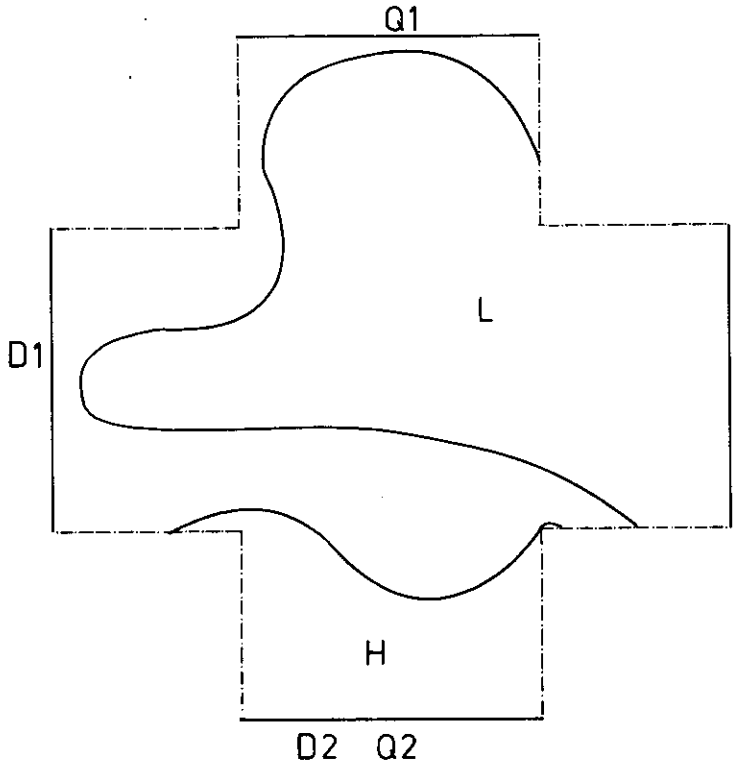
Q1
L
D1
H
D2
Q2

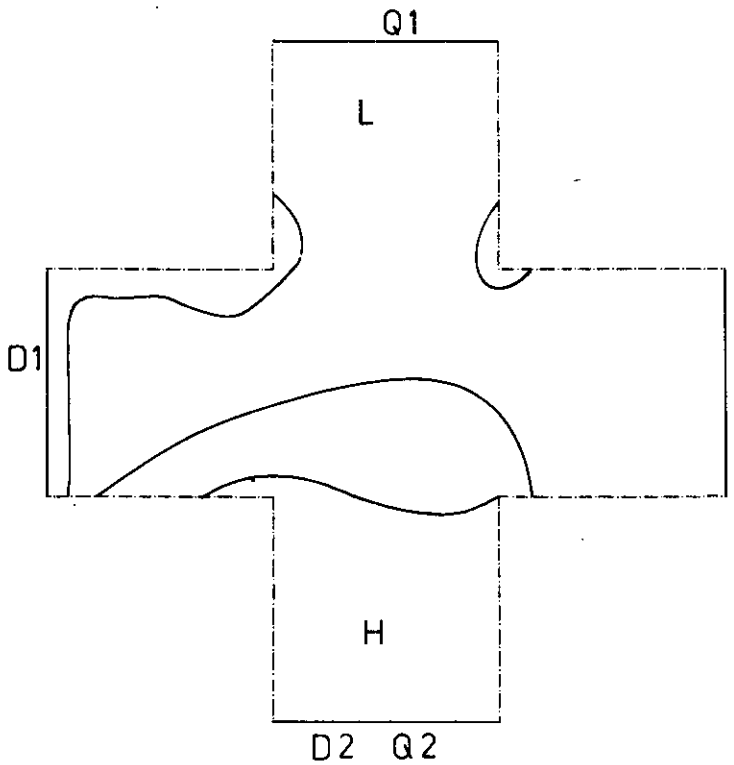
Q1
L
D1
H
D2
Q2

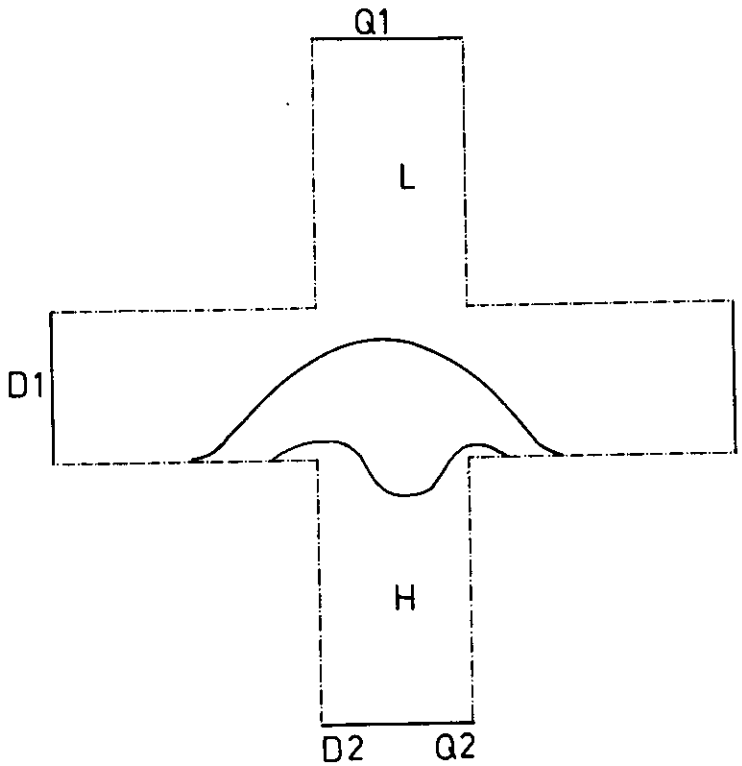
Q1
L
D1
H
D2
Q2

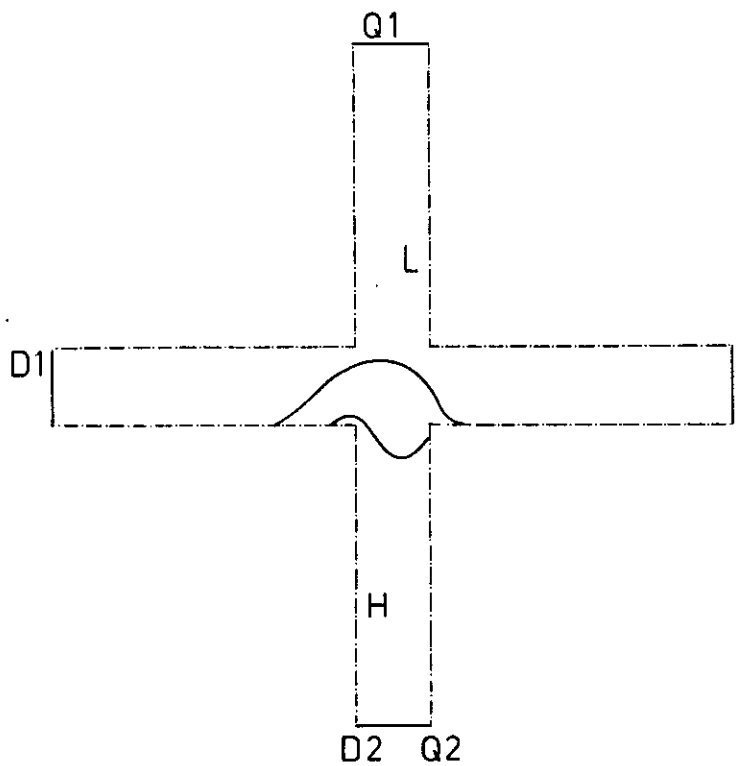
Q1
L
D1
H
D2
Q2

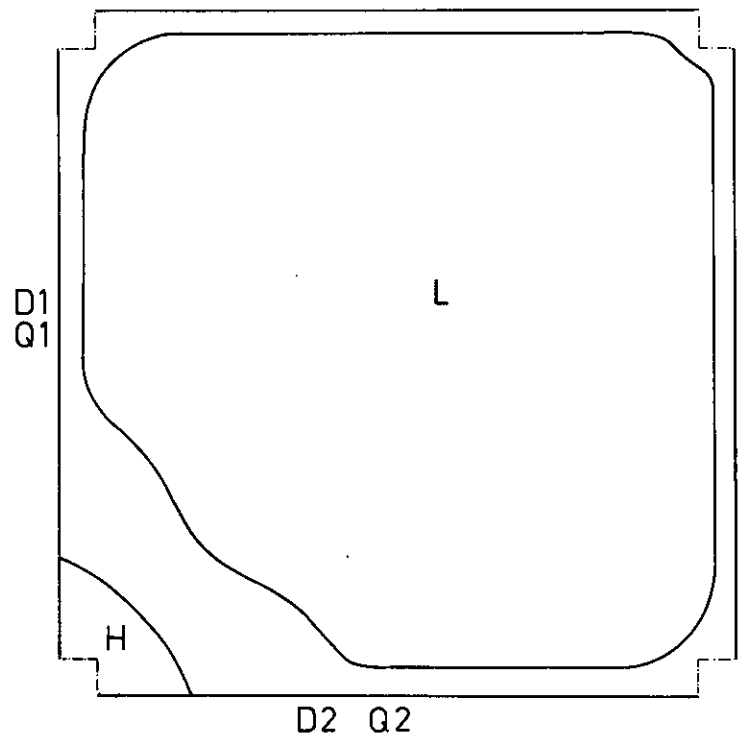
D1
Q1
L
H
D2 Q2

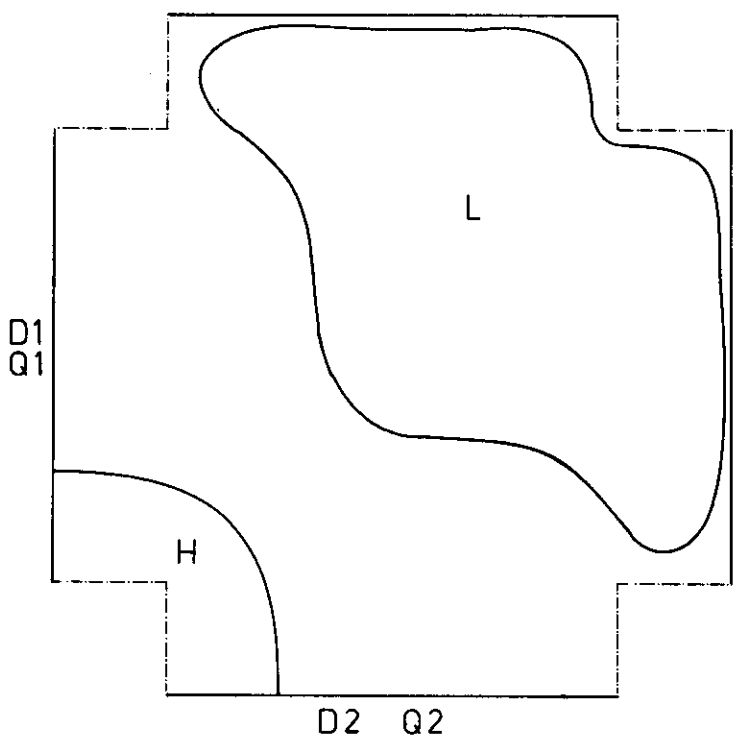
L
D1
Q1
H
D2 Q2

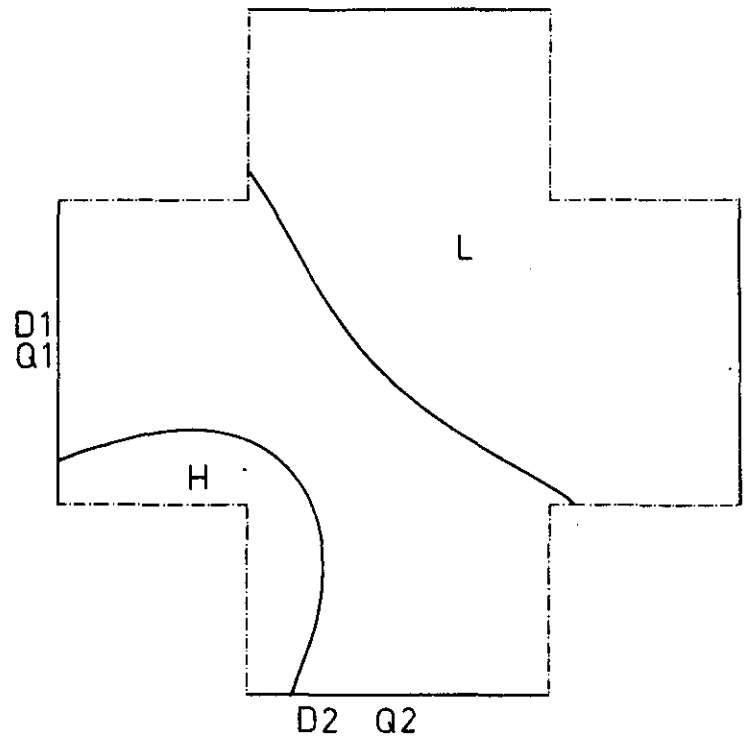
L
D1
Q1
H
D2 Q2

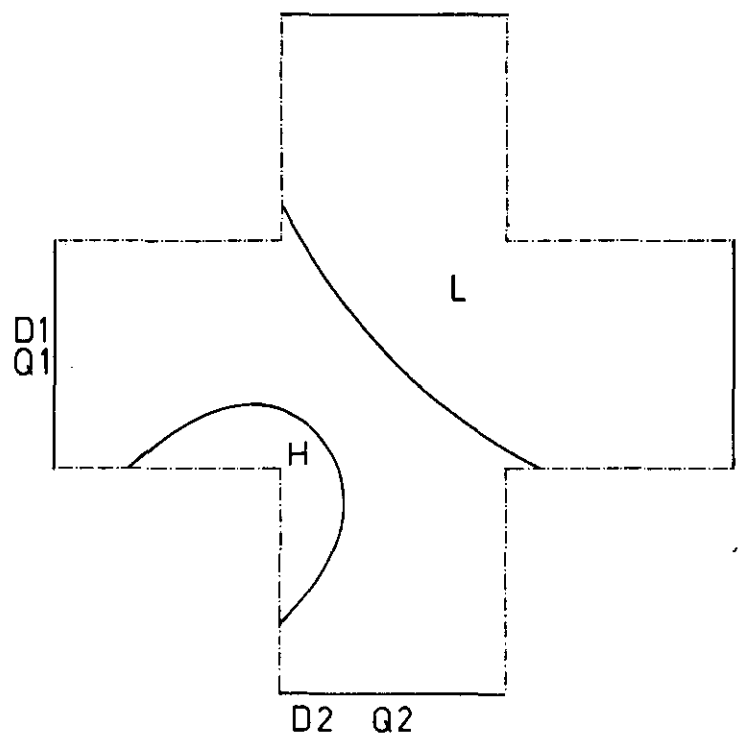
L
D1
Q1
H
D2 Q2

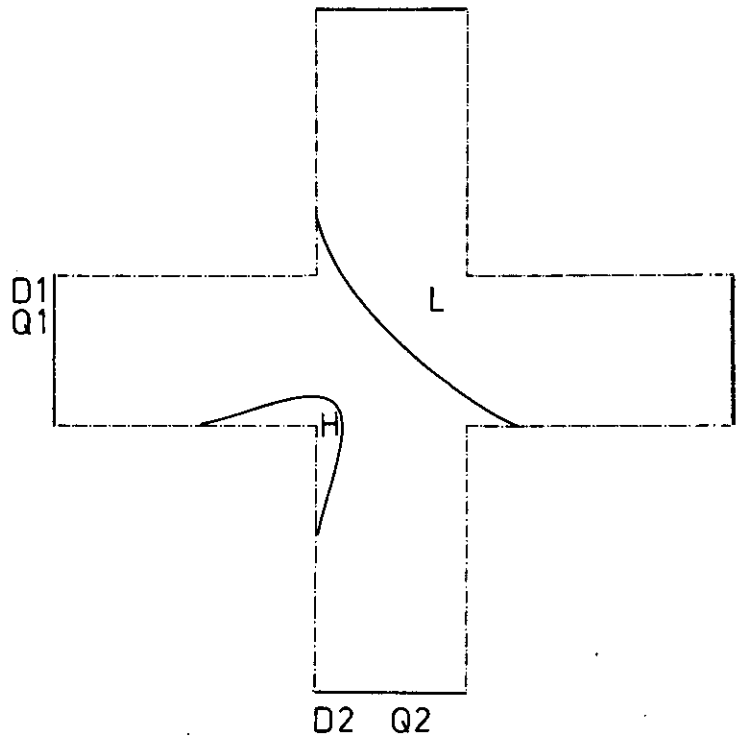
D1
Q1
L
H
D2 Q2

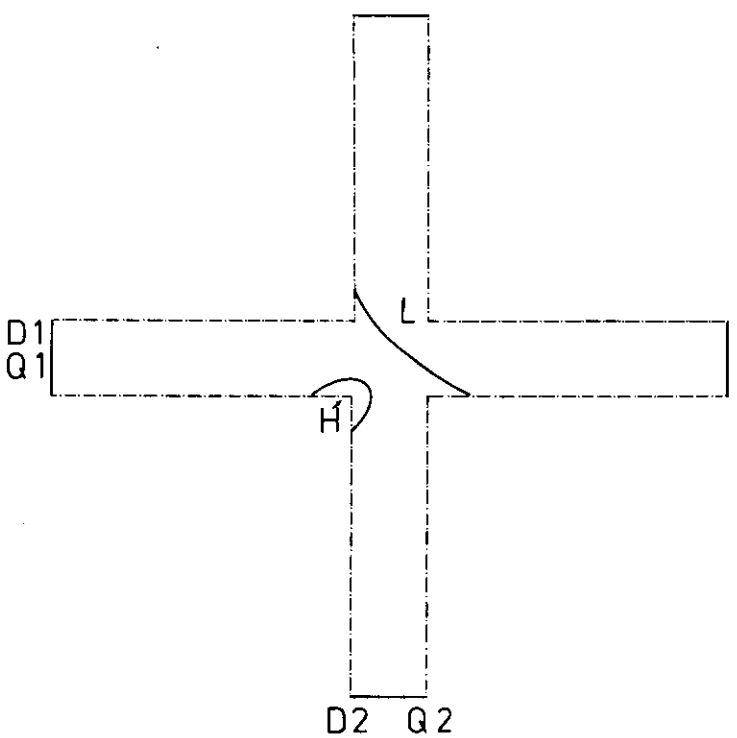
L
D1
Q1
H
D2 Q2

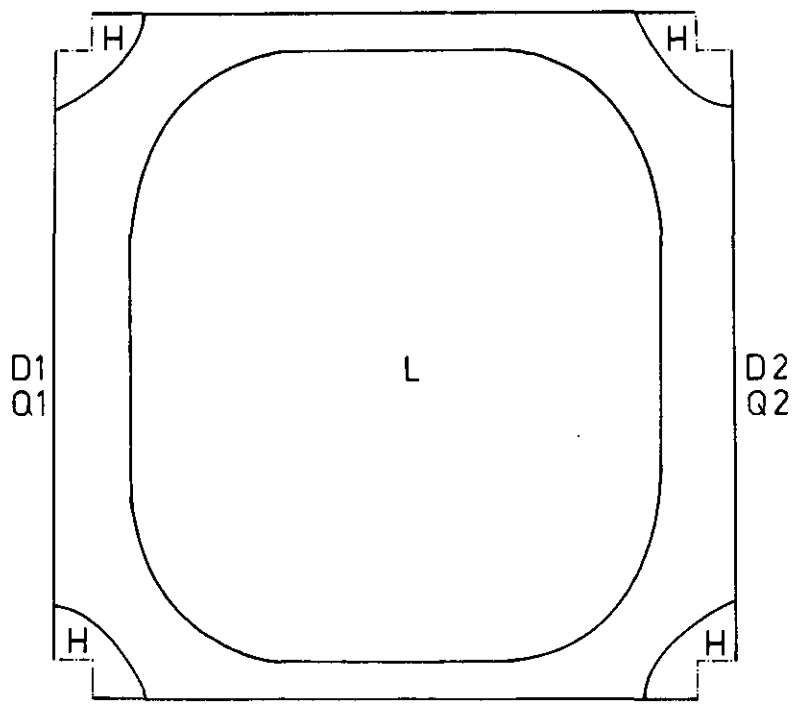
H
H
D1
Q1
L
D2
Q2
H
H

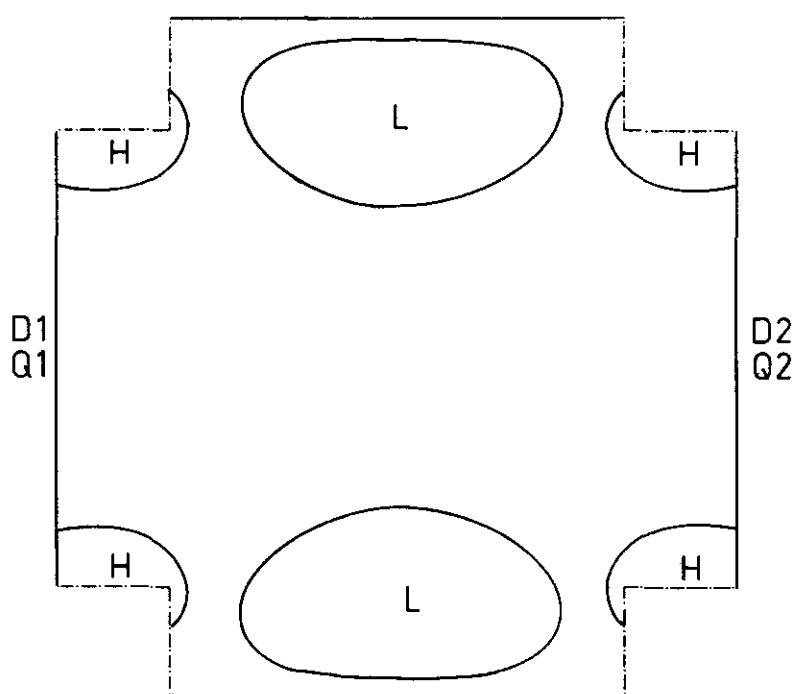
L
H
H
D1
Q1
D2
Q2
H
H
L

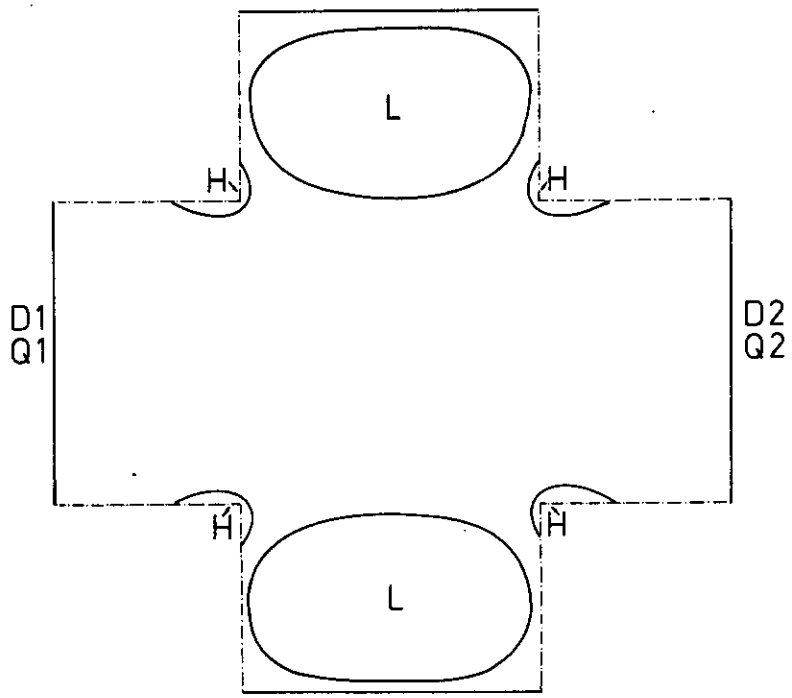
L
H
H
D1
Q1
D2
Q2
H
H
L

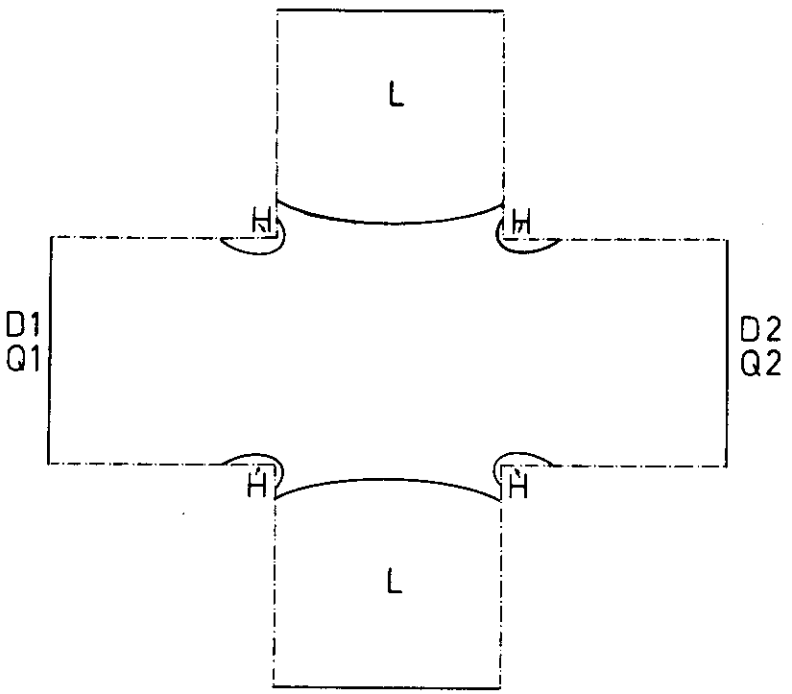
L
H
H
D1
Q1
D2
Q2
H
H
L

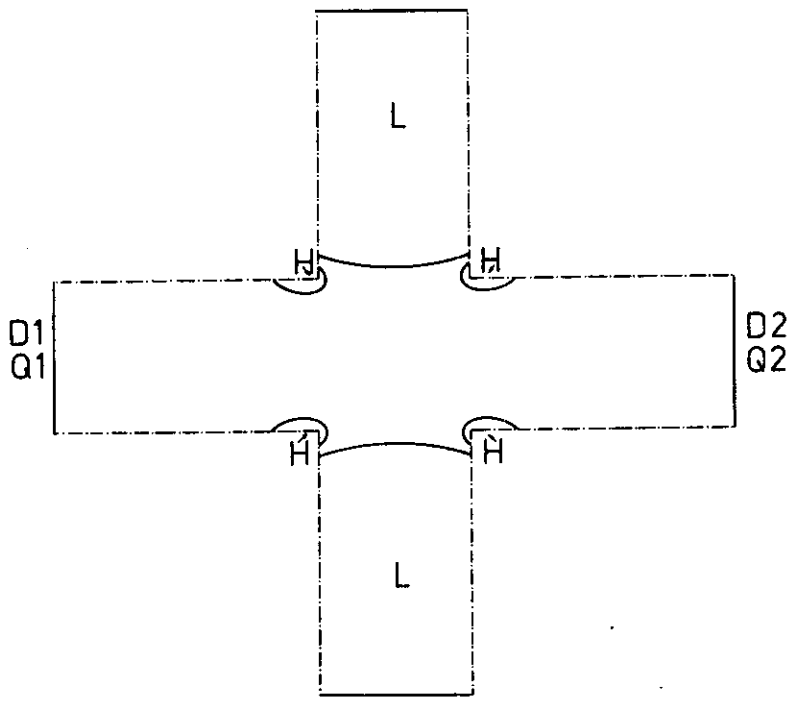
L
H
H
D1
Q1
D2
Q2
H
H
L

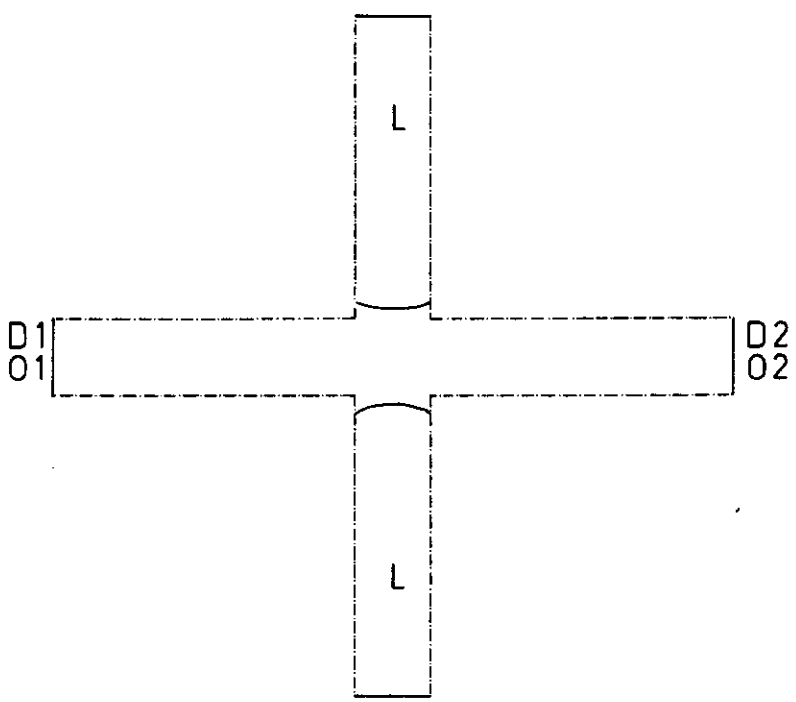
L
D1
O1
D2
O2
L

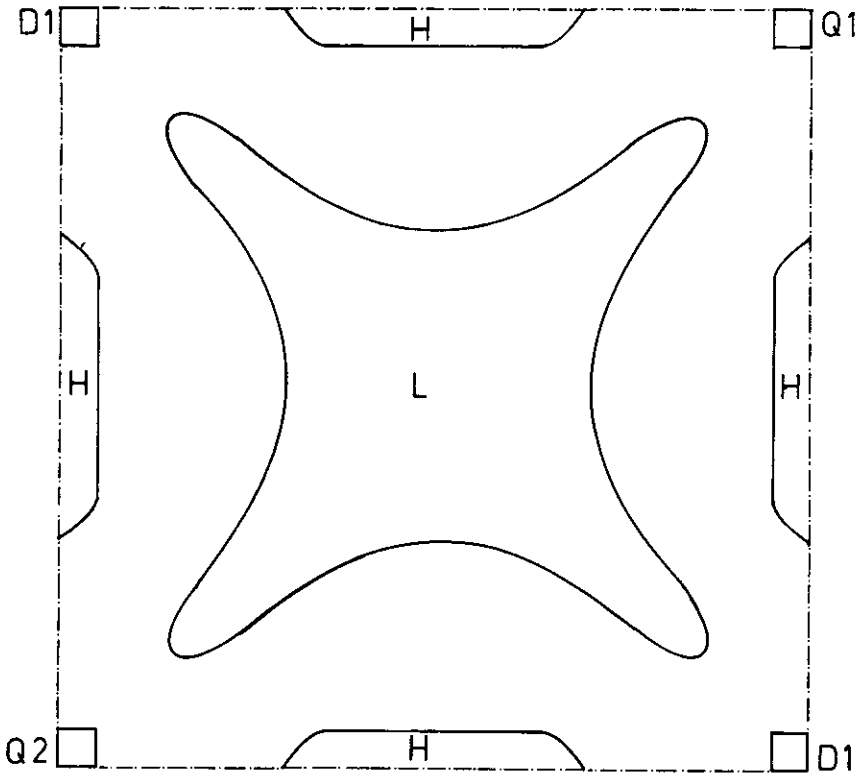
D1
H
Q1
H
L
H
Q2
H
D1

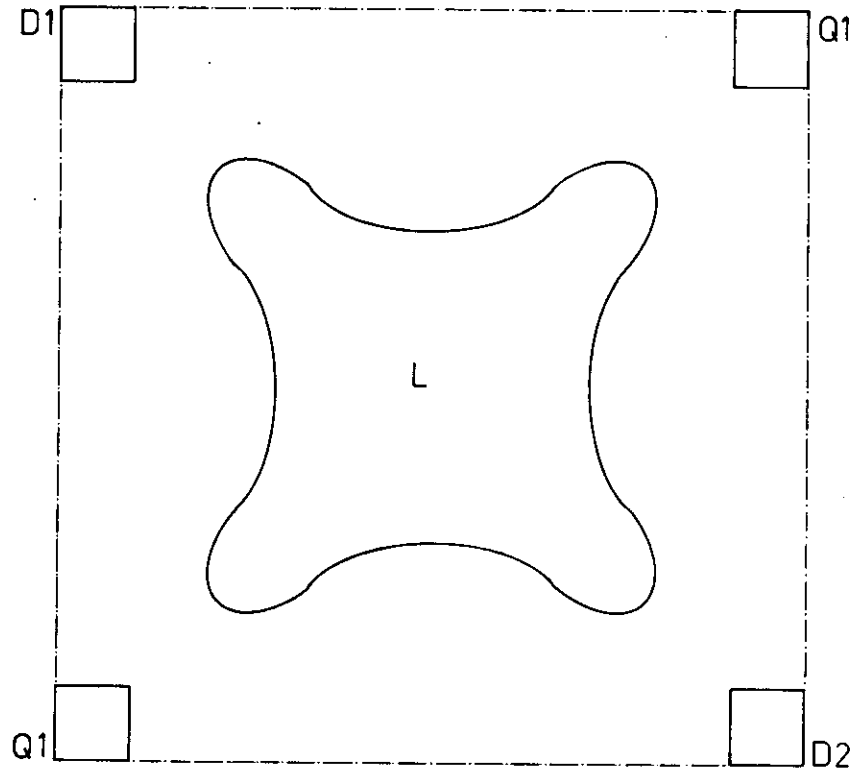
D1
Q1
L
Q1
D2

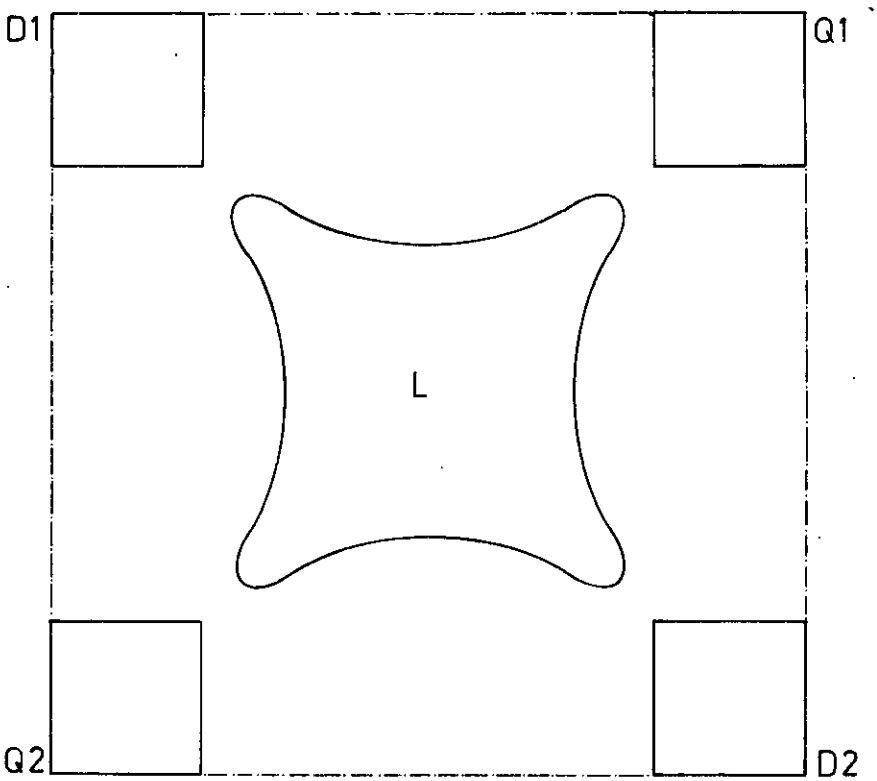
D1
Q1
L
Q2
D2

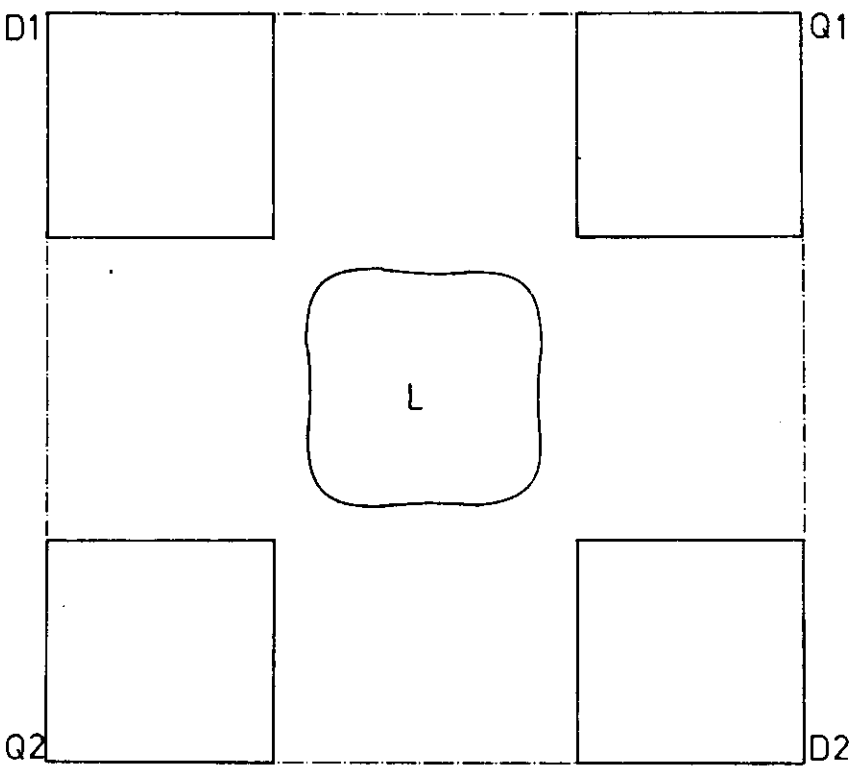
D1
Q1
L
Q2
D2

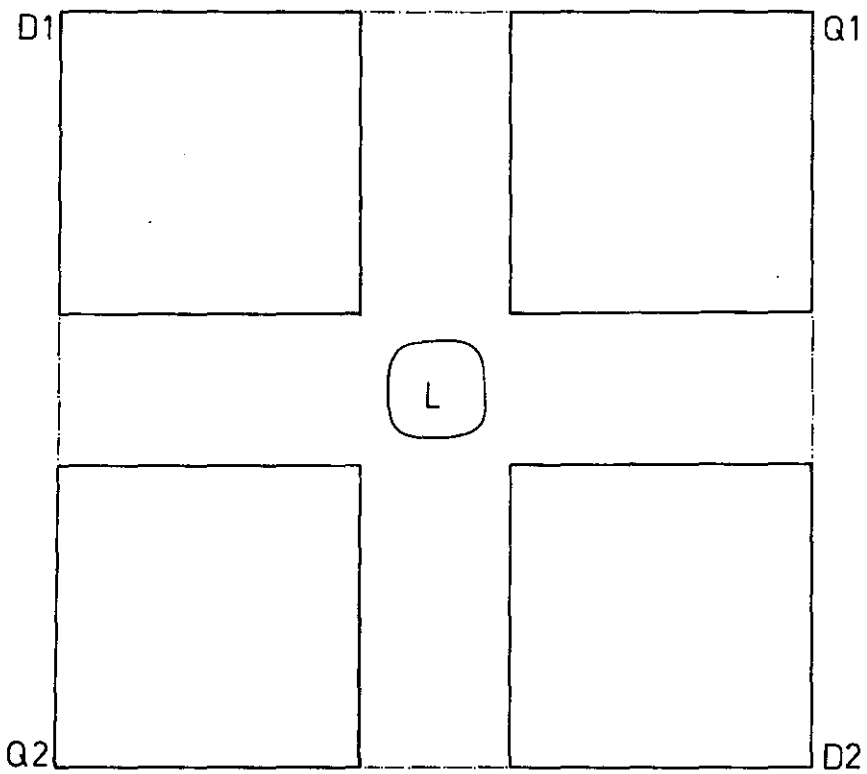
D1
Q1
L
Q2
D2

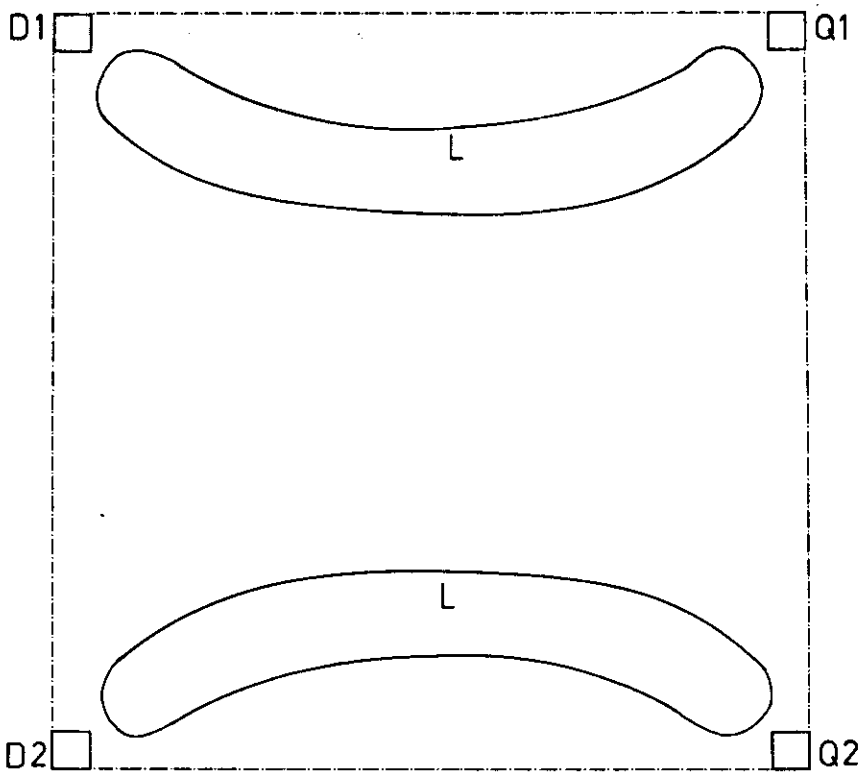
D1
Q1
L
L
D2
Q2

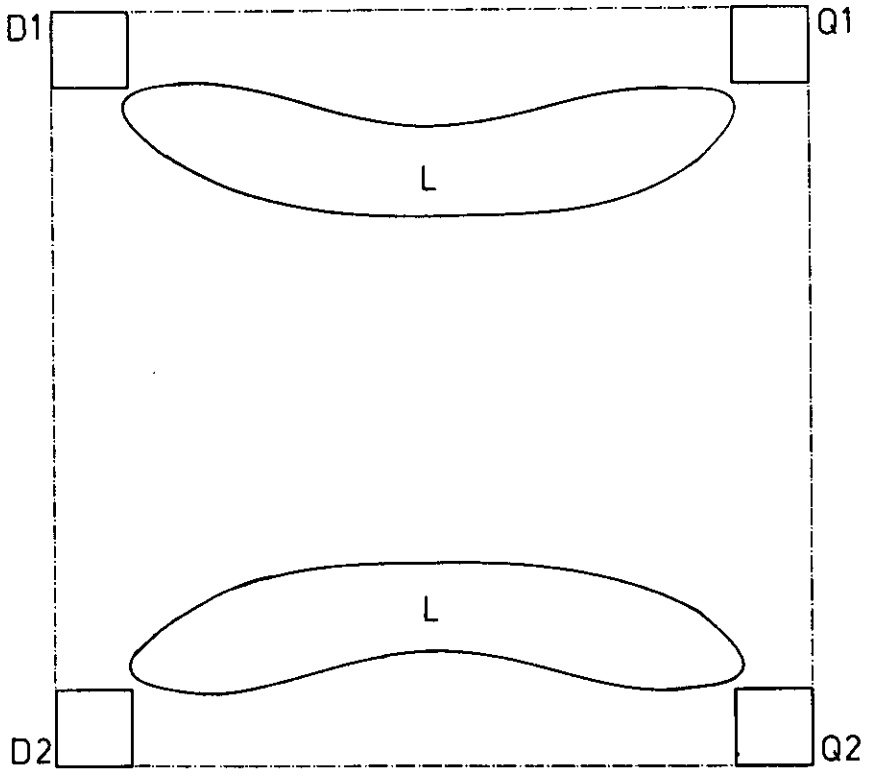
D1
Q1
L
L
D2
Q2

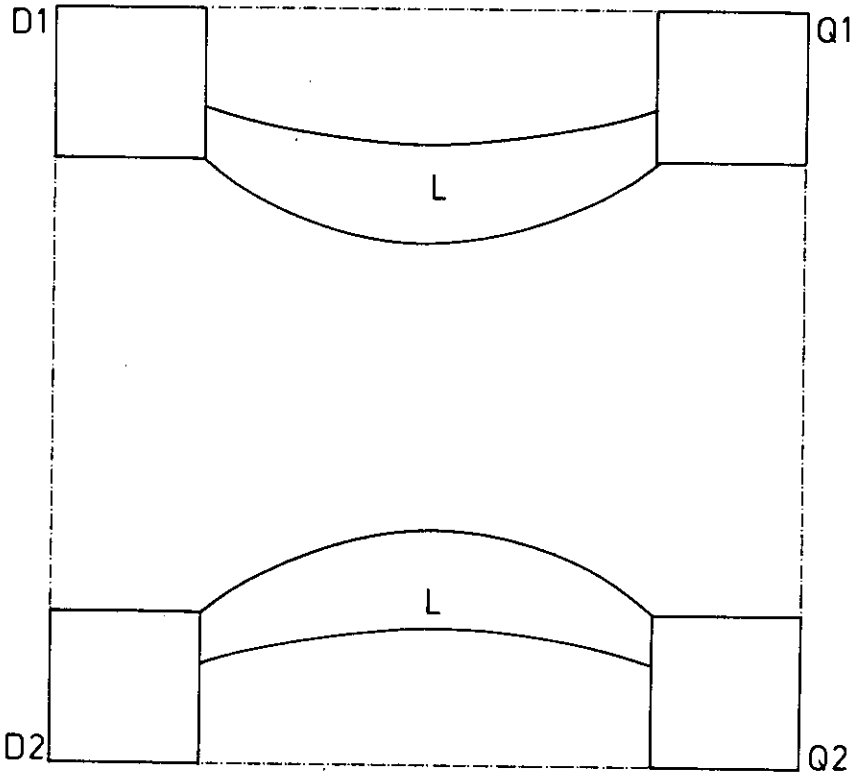
D1
Q1
L
L
D2
Q2

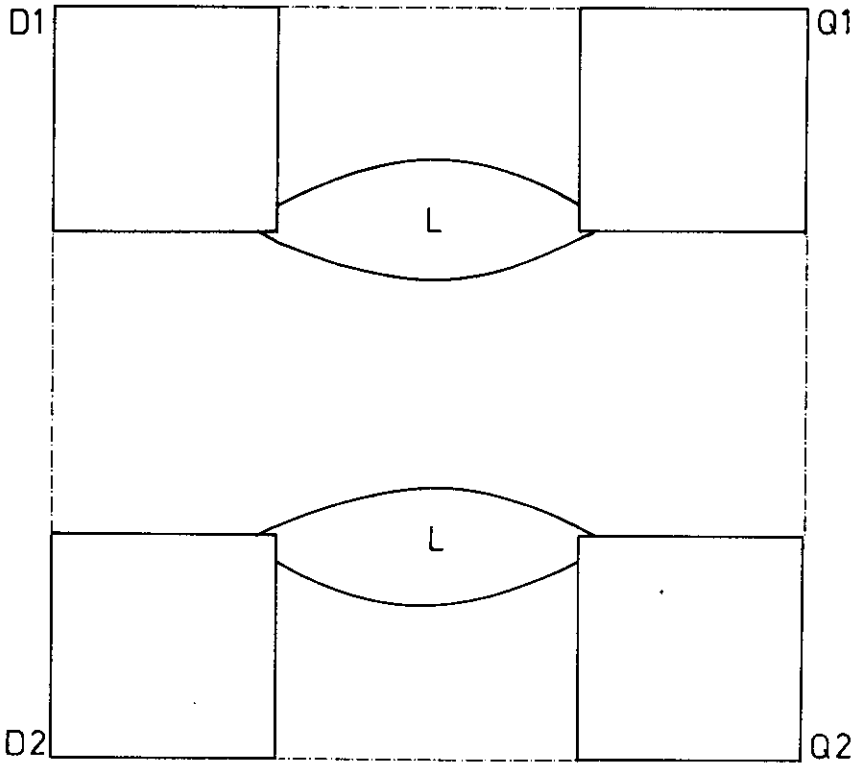
D1
Q1
L
L
D2
Q2

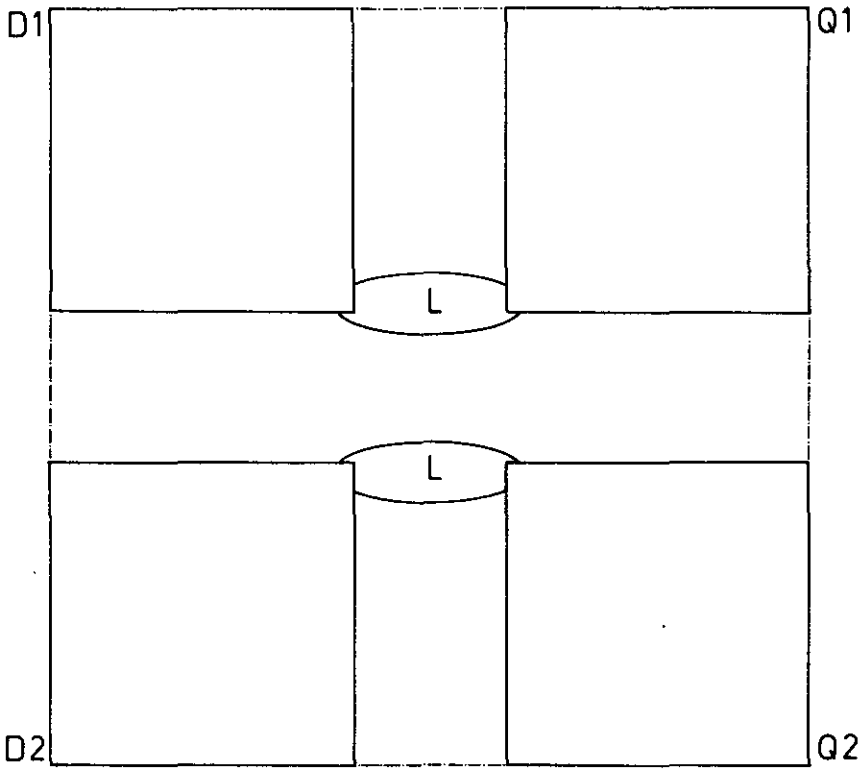
D1
Q1
L
L
D2
Q2

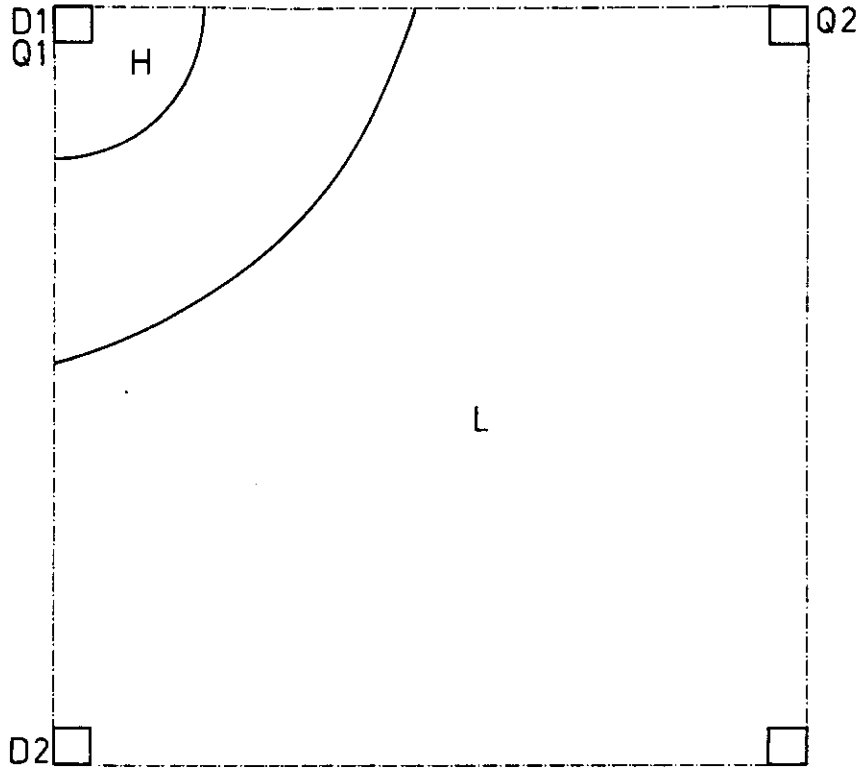
D1
Q1
H
Q2
L
D2

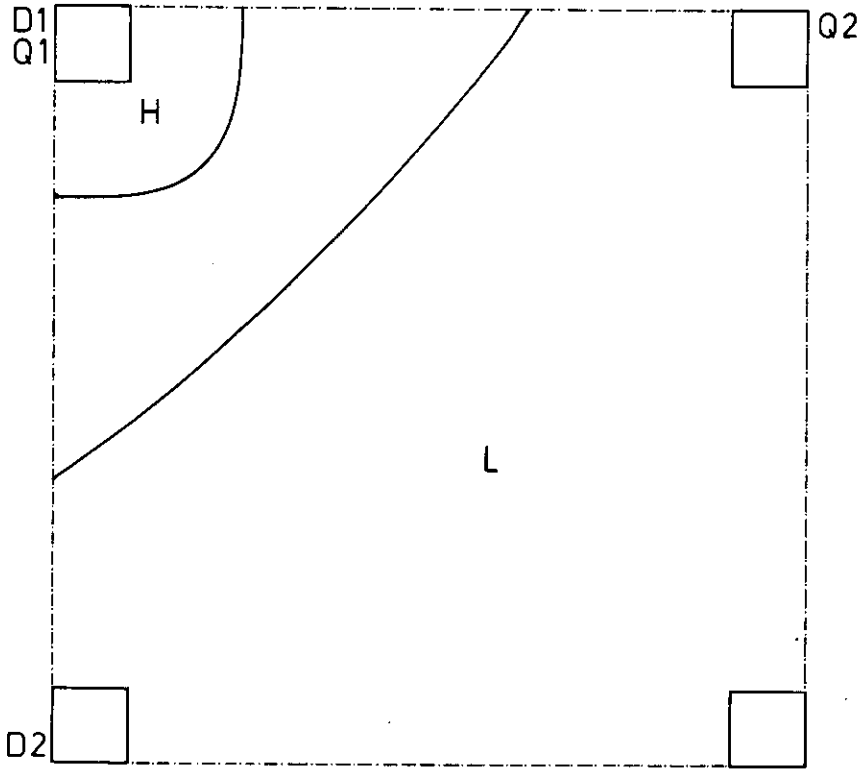
D1
Q1
H
Q2
L
D2

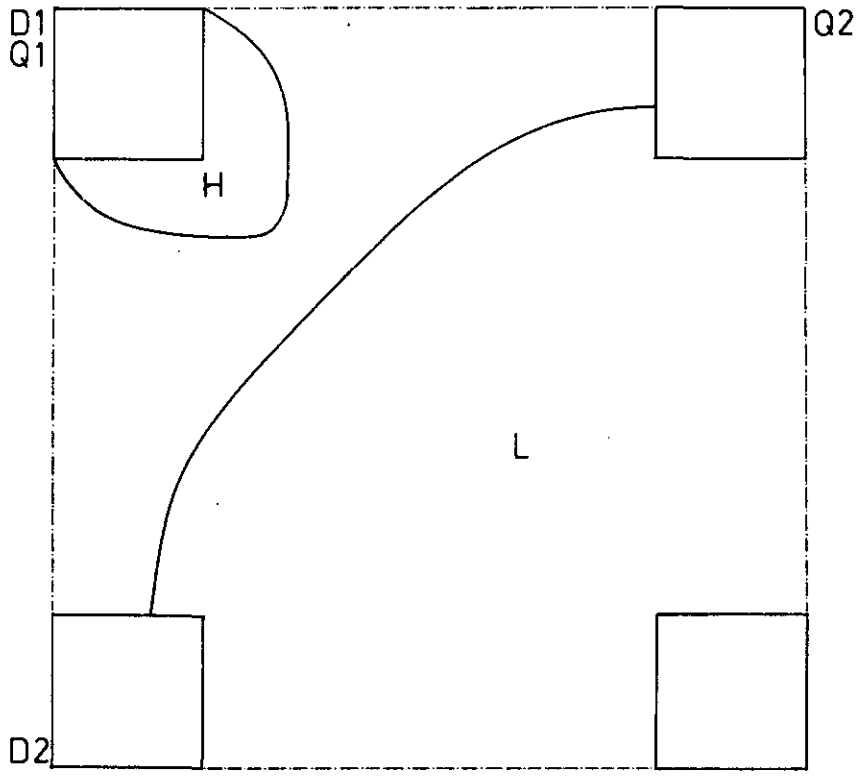
D1
Q1
Q2
H
L
D2

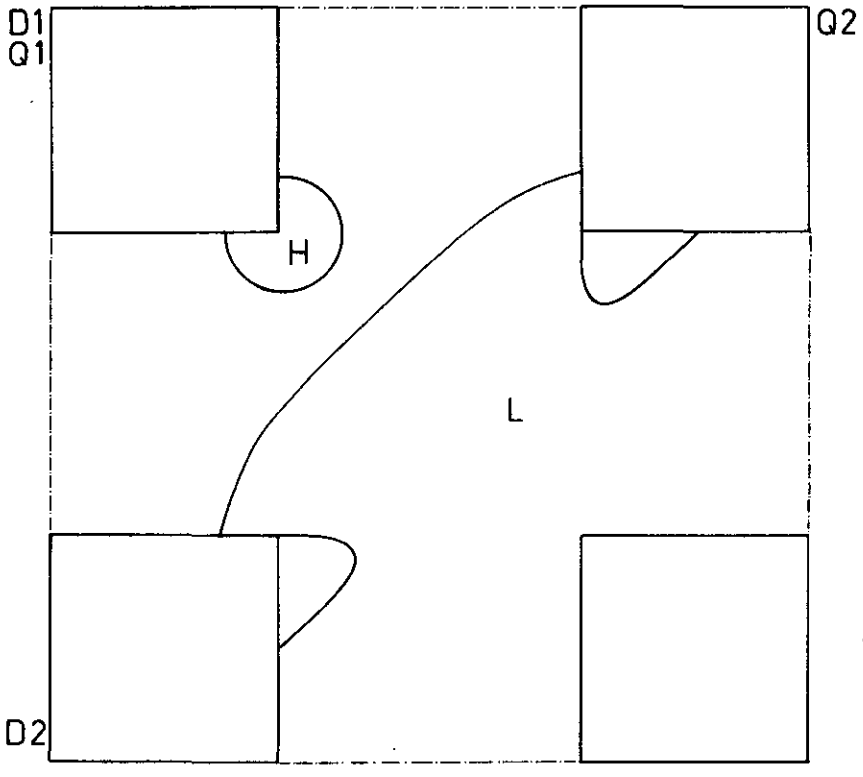
D1
Q1
Q2
H
L
D2

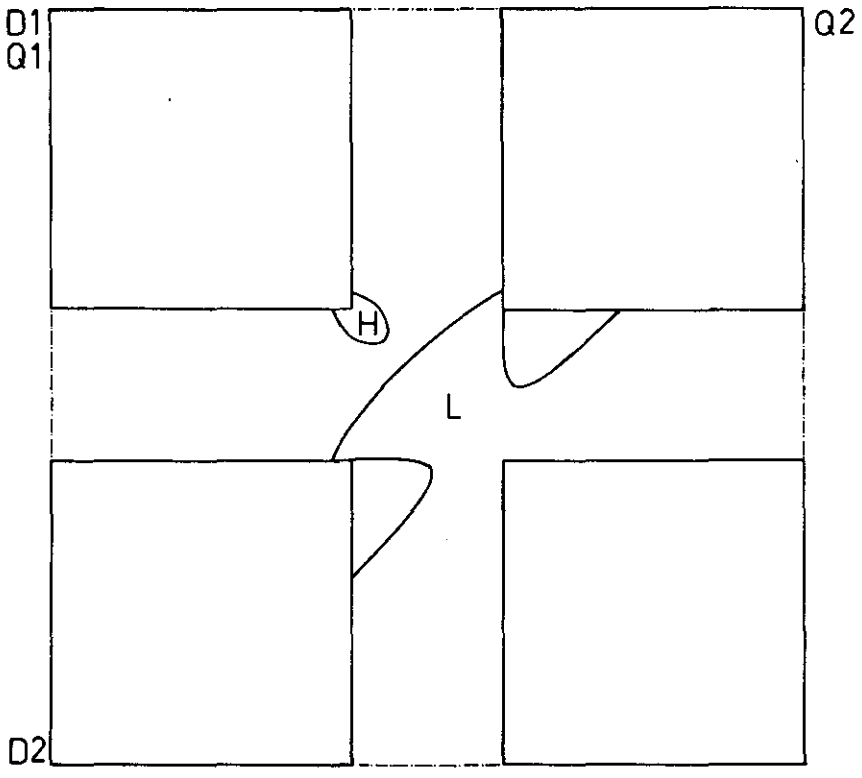
D1
Q1
Q2
H
L
D2

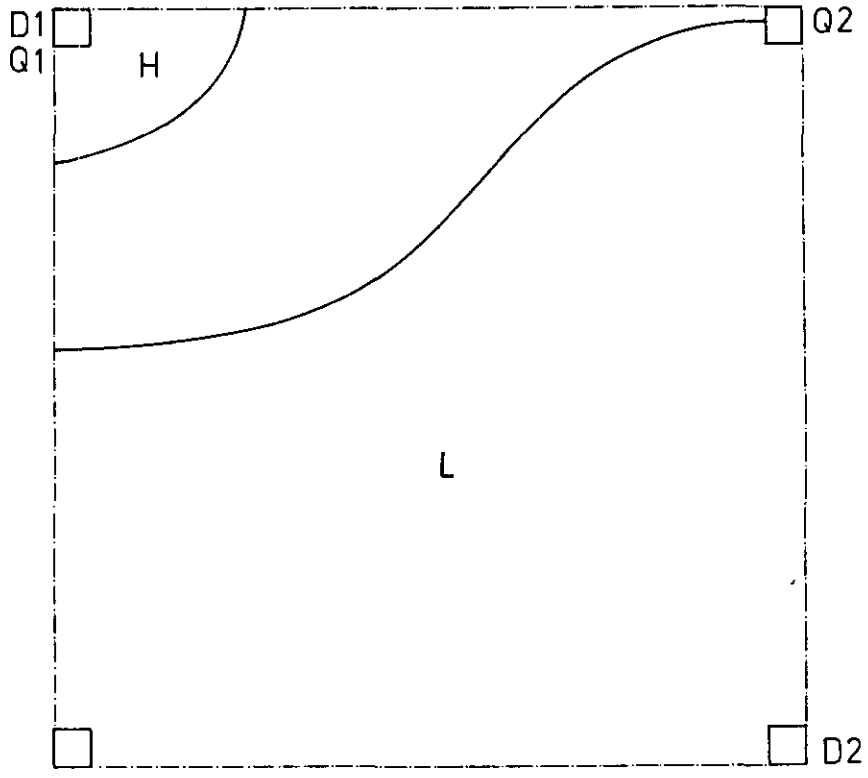
D1
Q1
H
Q2
L
D2

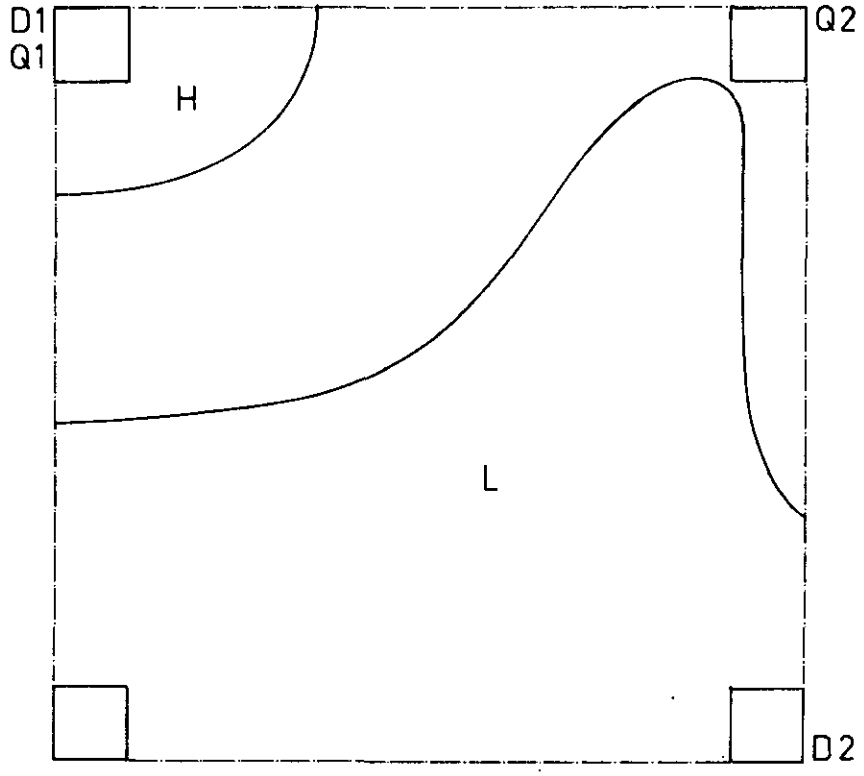
D1
Q1
H
Q2
L
D2

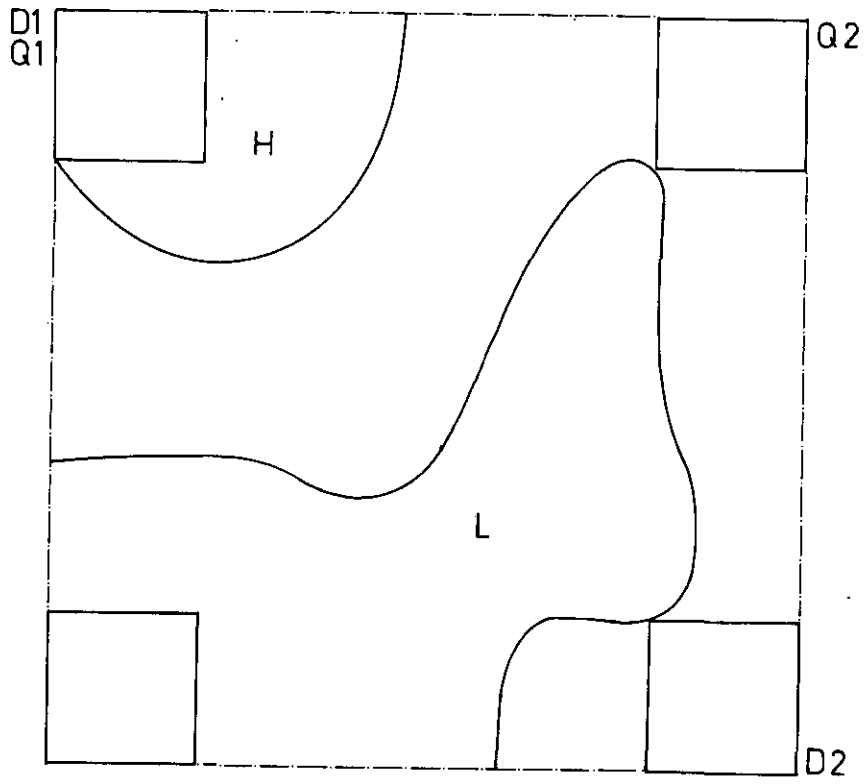
D1
Q1
Q2
H
L
D2

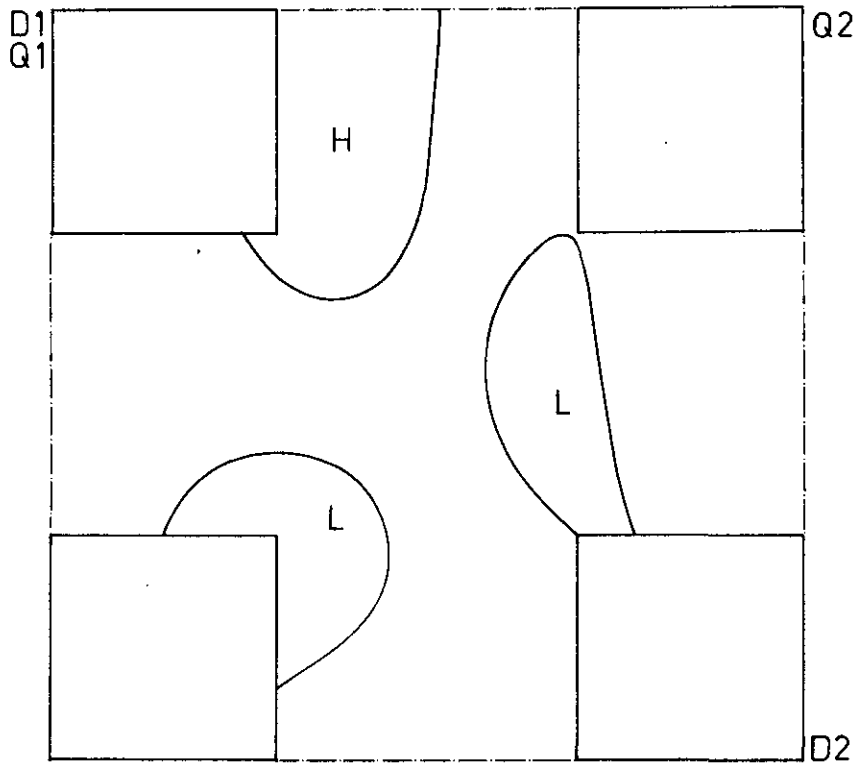
D1
Q1
Q2
H
L
L
D2

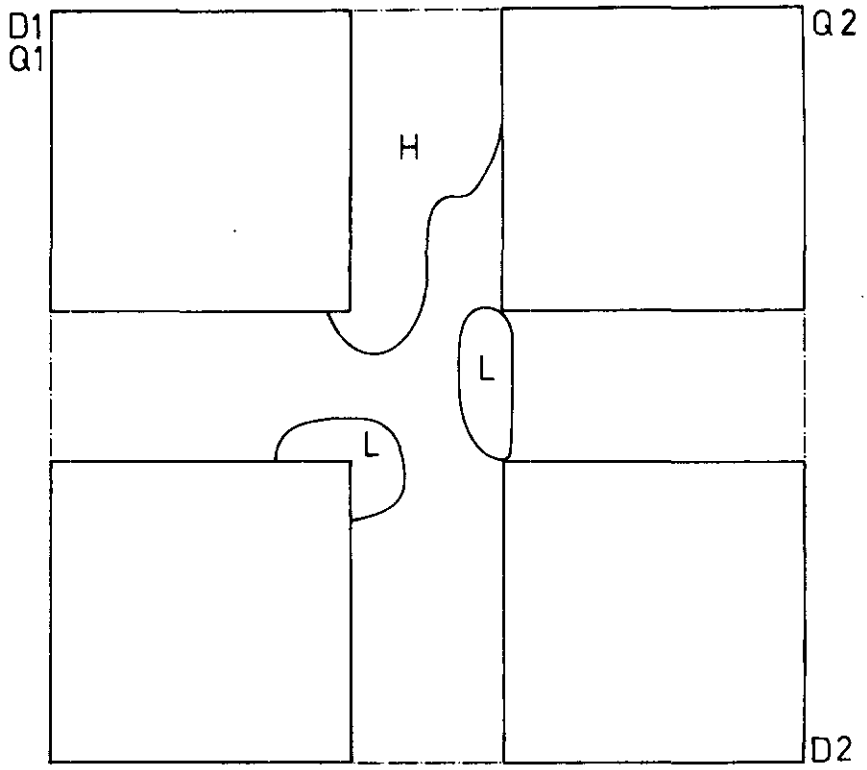
D1
Q1
H
Q2
L
L
D2

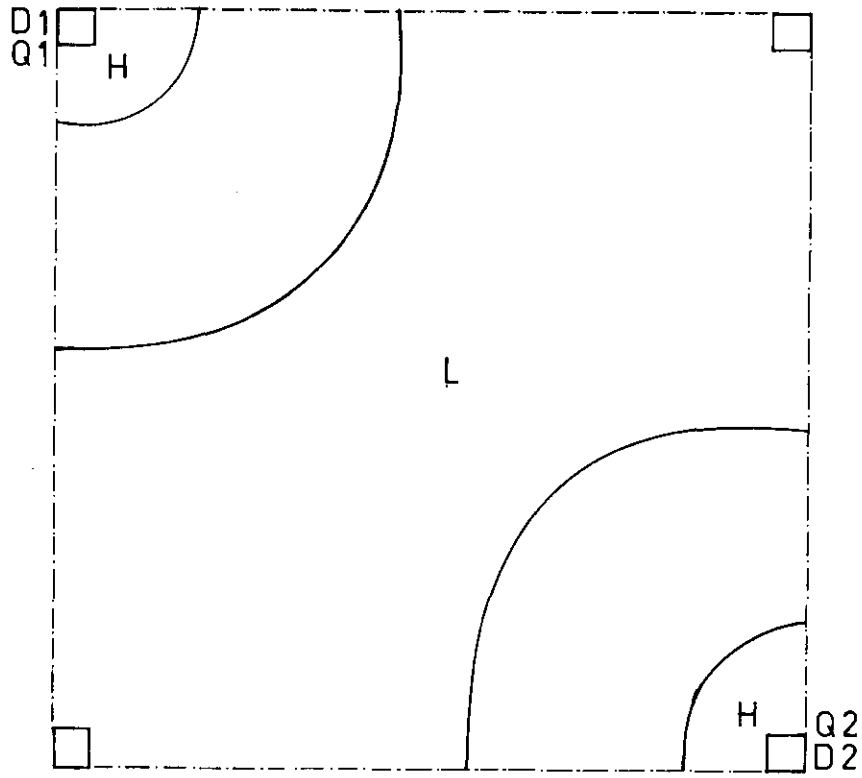
D1
Q1
H
L
H
Q2
D2

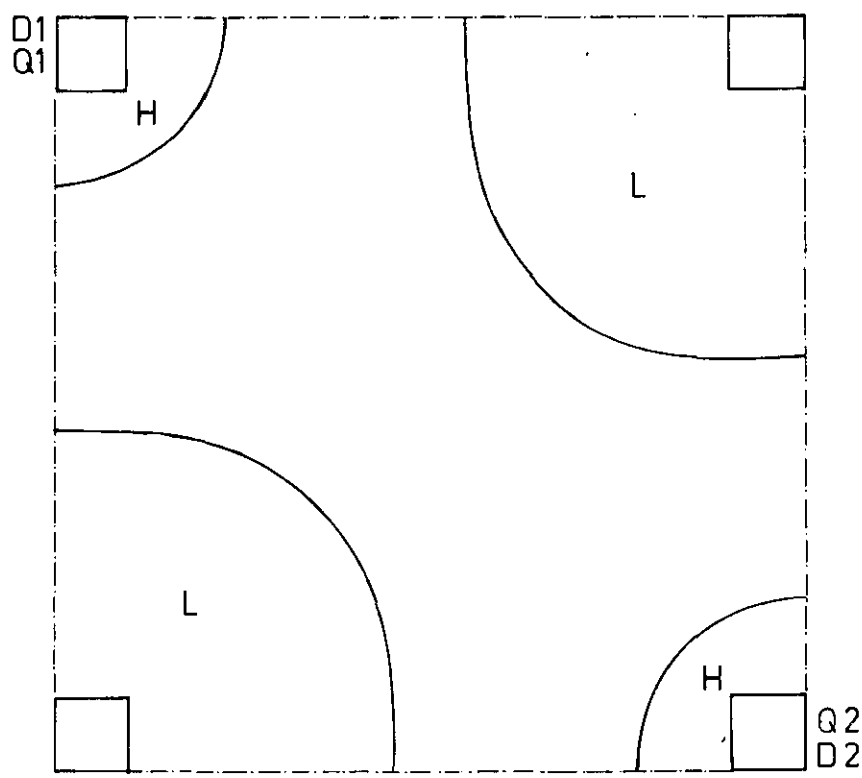
D1
Q1
H
L
L
H
Q2
D2

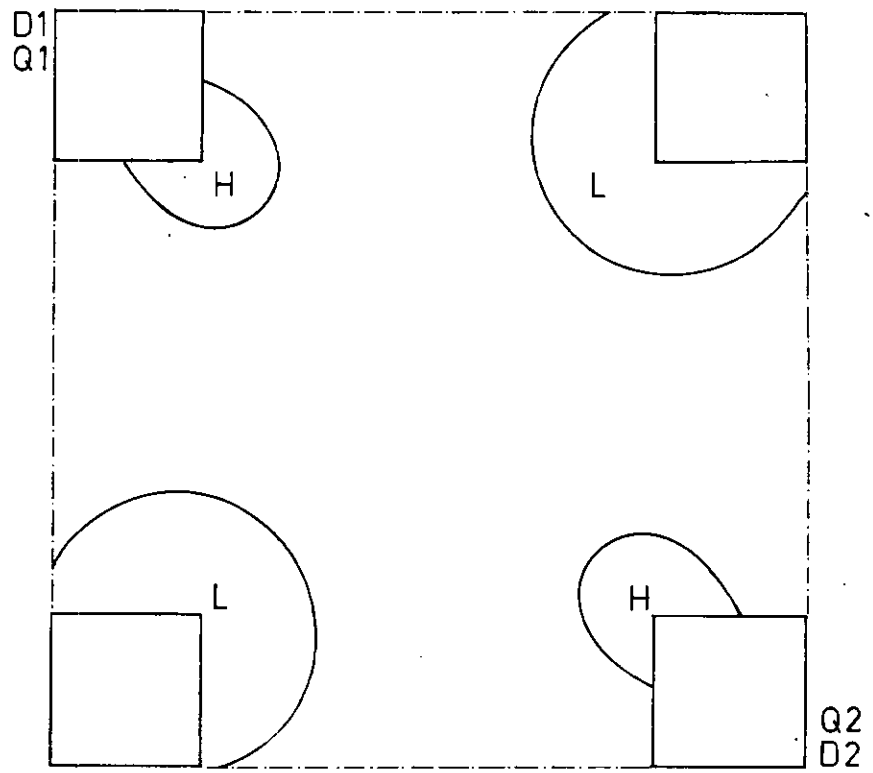
D1
Q1
H
L
L
H
Q2
D2

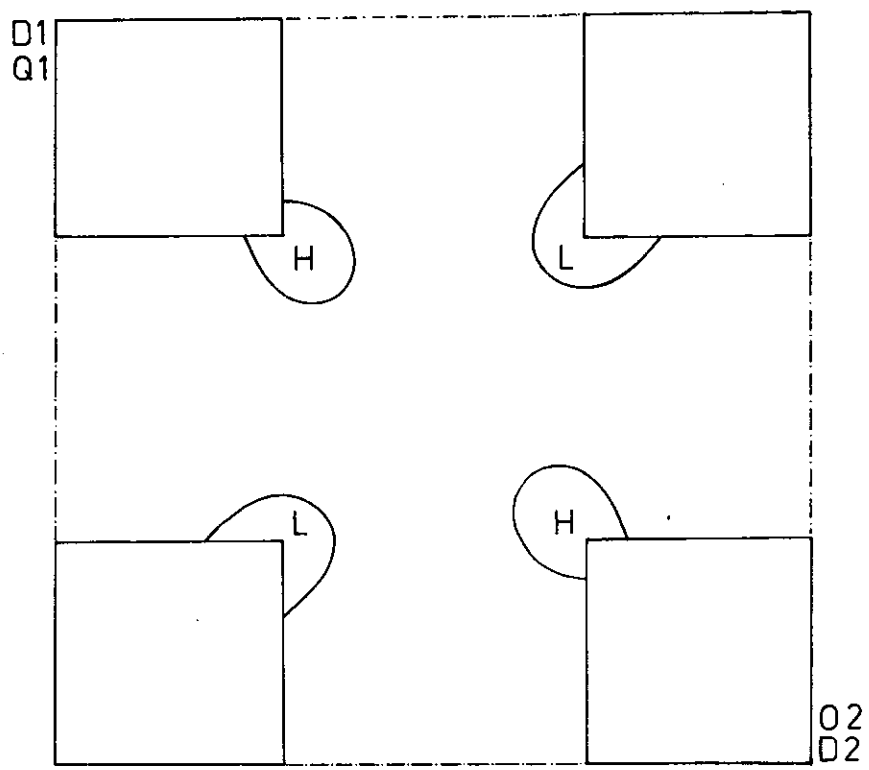
D1
Q1
H
L
L
H
Q2
D2

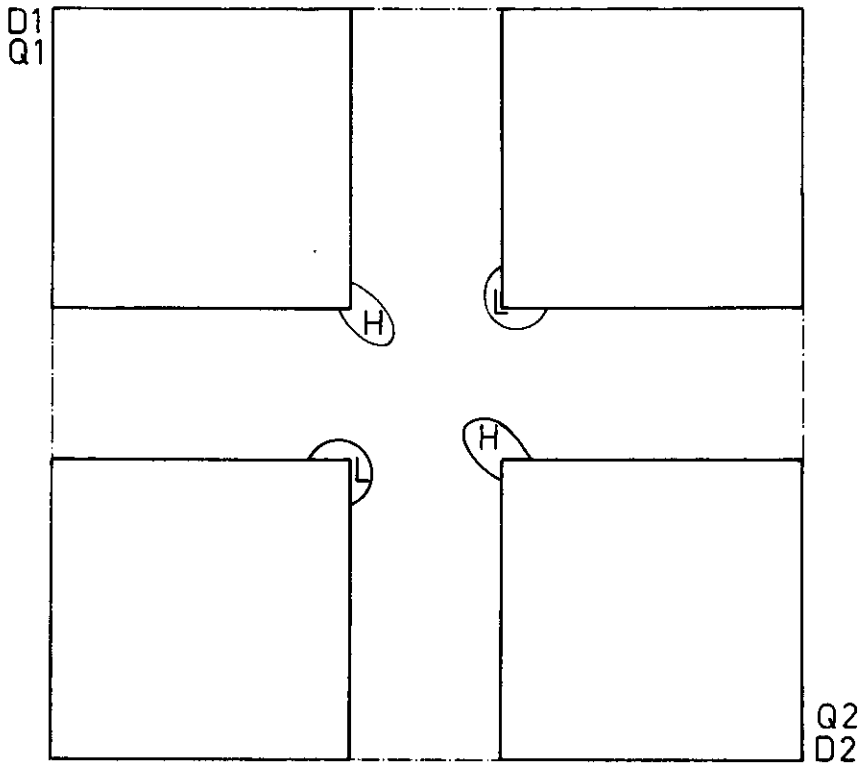
D1
Q1
H
L
L
H
Q2
D2

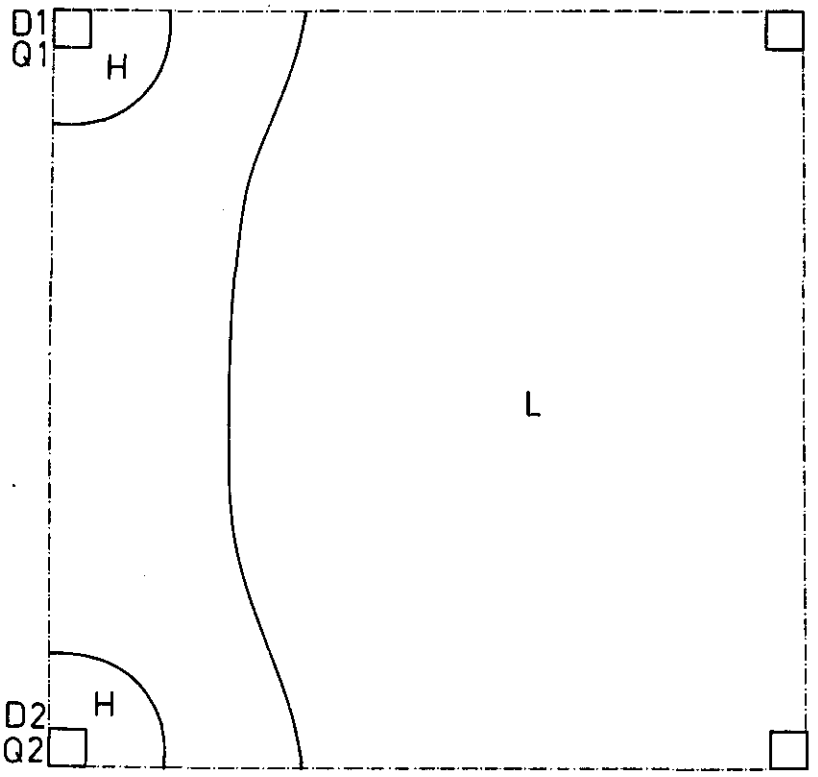
D1
Q1
H
L
H
D2
Q2

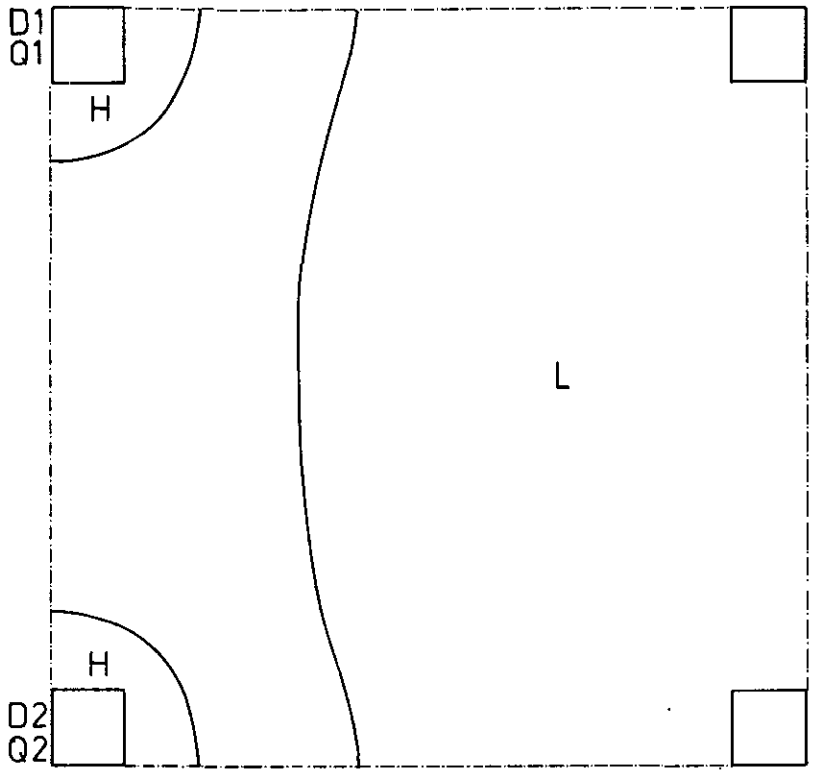
D1
Q1
H
L
H
D2
Q2

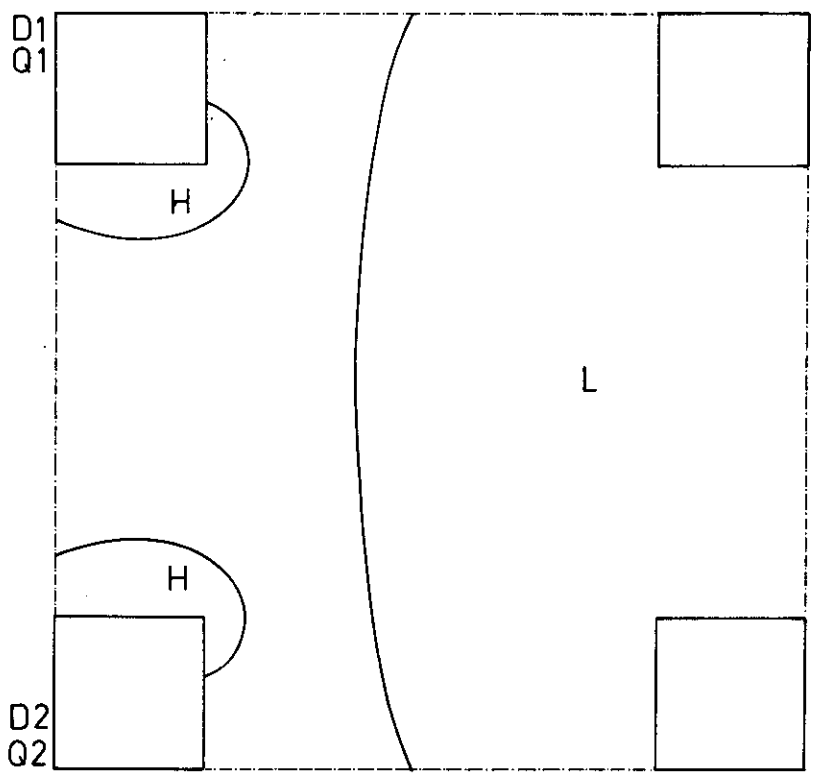
D1
Q1
H
L
H
D2
Q2

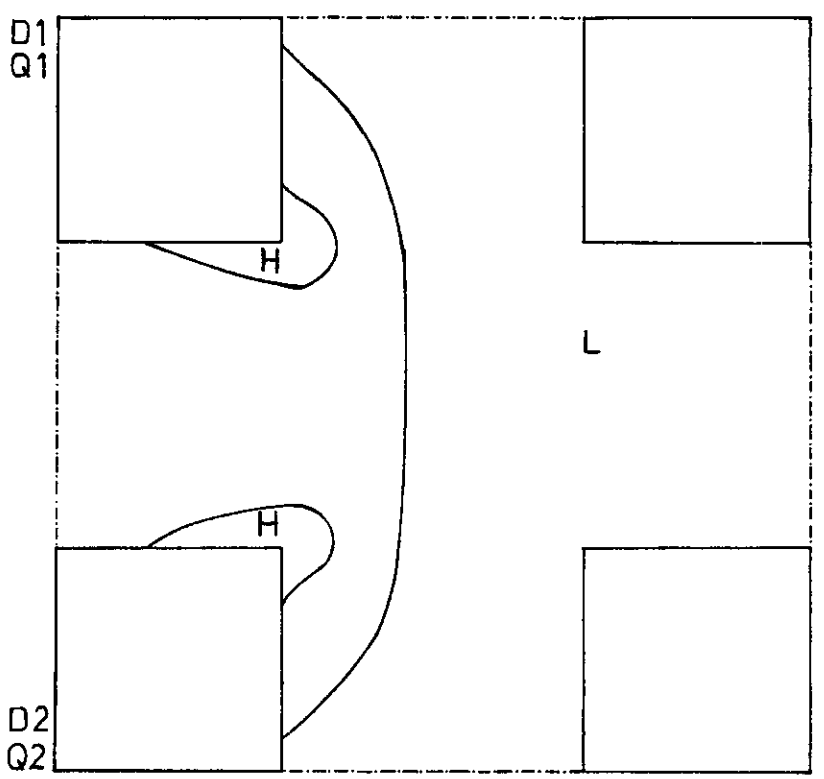
D1
Q1
H
L
H
D2
Q2

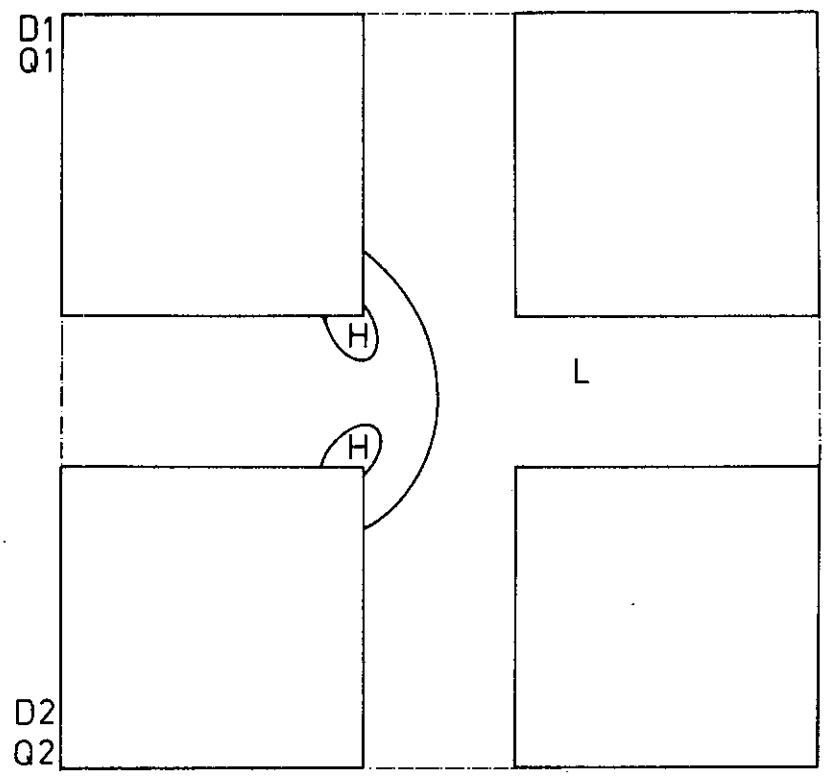
D1
Q1
H
H
L
D2
Q2

EINDHOVEN UNIVERSITY OF TECHNOLOGY
THE NETHERLANDS
DEPARTMENT OF ELECTRICAL ENGINEERING

Reports:

1) **Dijk, J., M. Jeuken and E.J. Maanders**
AN ANTENNA FOR A SATELLITE COMMUNICATION GROUND STATION (PROVISIONAL ELECTRICAL DESIGN).
TH-Report 68-E-01. 1968. ISBN 90-6144-001-7

2) **Veefkind, A., J.H. Blom and L.H.Th. Rietjens**
THEORETICAL AND EXPERIMENTAL INVESTIGATION OF A NON-EQUILIBRIUM PLASMA IN A MHD CHANNEL. Submitted to the Symposium on Magnetohydrodynamic Electrical Power Generation, Warsaw, Poland, 24-30 July, 1968.
TH-Report 68-E-02. 1968. ISBN 90-6144-002-5

3) **Boom, A.J.W. van den and J.H.A.M. Melis**
A COMPARISON OF SOME PROCESS PARAMETER ESTIMATING SCHEMES.
TH-Report 68-E-03. 1968. ISBN 90-6144-003-3

4) **Eykhoff, P., P.J.M. Ophey, J. Severs and J.O.M. Oome**
AN ELECTROLYTIC TANK FOR INSTRUCTIONAL PURPOSES REPRESENTING THE COMPLEX-FREQUENCY PLANE.
TH-Report 68-E-02. 1968. ISBN 90-6144-004-1

5) **Vermij, L. and J.E. Daalder**
ENERGY BALANCE OF FUSING SILVER WIRES SURROUNDED BY AIR.
TH-Report 68-E-05. 1968. ISBN 90-6144-005-X

6) **Houben, J.W.M.A. and P. Massee**
MHD POWER CONVERSION EMPLOYING LIQUID METALS.
TH-Report 69-E-06. 1969. ISBN 90-6144-006-8

7) **Heuvel, W.M.C. van den and W.F.J. Kersten**
VOLTAGE MEASUREMENT IN CURRENT ZERO INVESTIGATIONS.
TH-Report 69-E-07. 1969. ISBN 90-6144-007-6

8) **Vermij, L.**
SELECTED BIBLIOGRAPHY OF FUSES.
TH-Report 69-E-08. 1969. ISBN 90-6144-008-4

9) **Westenberg, J.Z.**
SOME IDENTIFICATION SCHEMES FOR NON-LINEAR NOISY PROCESSES.
TH-Report 69-E-09. 1969. ISBN 90-6144-009-2

10) **Koop, H.E.M., J. Dijk and E.J. Maanders**
ON CONICAL HORN ANTENNAS.
TH-Report 70-E-10. 1970. ISBN 90-6144-010-6

11) **Veefkind, A.**
NON-EQUILIBRIUM PHENOMENA IN A DISC-SHAPED MAGNETOHYDRODYNAMIC GENERATOR.
TH-Report 70-E-11. 1970. ISBN 90-6144-011-4

12) **Jansen, J.K.M., M.E.J. Jeuken and C.W. Lamerechtse**
THE SCALAR FEED.
TH-Report 70-E-12. 1969. ISBN 90-6144-012-2

13) **Teuling, D.J.A.**
ELECTRONIC IMAGE MOTION COMPENSATION IN A PORTABLE TELEVISION CAMERA.
TH-Report 70-E-13. 1970. ISBN 90-6144-013-0

EINDHOVEN UNIVERSITY OF TECHNOLOGY
THE NETHERLANDS
DEPARTMENT OF ELECTRICAL ENGINEERING

Reports:

14) Lorencin, M.
AUTOMATIC METEOR REFLECTIONS RECORDING EQUIPMENT.
TH-Report 70-E-14. 1970. ISBN 90-6144-014-9

15) Smets, A.S.
THE INSTRUMENTAL VARIABLE METHOD AND RELATED IDENTIFICATION SCHEMES.
TH-Report 70-E-15. 1970. ISBN 90-6144-015-7

16) White, Jr., R.C.
A SURVEY OF RANDOM METHODS FOR PARAMETER OPTIMIZATION.
TH-Report 70-E-16. 1971. ISBN 90-6144-016-5

17) Talmon, J.L.
APPROXIMATED GAUSS-MARKOV ESTIMATORS AND RELATED SCHEMES.
TH-Report 71-E-17. 1971. ISBN 90-6144-017-3

18) Kalášek, V.
MEASUREMENT OF TIME CONSTANTS ON CASCADE D.C. ARC IN NITROGEN.
TH-Report 71-E-18. 1971. ISBN 90-6144-018-1

19) Hosselet, L.M.L.F.
OZONBILDUNG MITTELS ELEKTRISCHER ENTLADUNGEN.
TH-Report 71-E-19. 1971. ISBN 90-6144-019-X

20) Arts, M.G.J.
ON THE INSTANTANEOUS MEASUREMENT OF BLOODFLOW BY ULTRASONIC MEANS.
TH-Report 71-E-20. 1971. ISBN 90-6144-020-3

21) Roer, Th.G. van de
NON-ISO THERMAL ANALYSIS OF CARRIER WAVES IN A SEMICONDUCTOR.
TH-Report 71-E-21. 1971. ISBN 90-6144-021-1

22) Jeuken, P.J., C. Huber and C.E.Mulders
SENSING INERTIAL ROTATION WITH TUNING FORKS.
TH-Report 71-E-22. 1971. ISBN 90-6144-022-X

23) Dijk, J., J.M. Berends and E.J. Maanders
APERTURE BLOCKAGE IN DUAL REFLECTOR ANTENNA SYSTEMS - A REVIEW.
TH-Report 71-E-23. 1971. ISBN 90-6144-023-8

24) Kregting, J. and R.C. White, Jr.
ADAPTIVE RANDOM SEARCH.
TH-Report 71-E-24. 1971. ISBN 90-6144-024-6

25) Damen, A.A.H. and H.A.L. Piceni
THE MULTIPLE DIPOLE MODEL OF THE VENTRICULAR DEPOLARISATION.
TH-Report 71-E-25. 1971. ISBN 90-6144-025-4

26) Bremmer, H.
A MATHEMATICAL THEORY CONNECTING SCATTERING AND DIFFRACTION PHENOMENA, INCLUDING BRAGG-TYPE INTERFERENCES.
TH-Report 71-E-26. 1971. ISBN 90-6144-026-2

27) Bokhoven, W.M.G. van
METHODS AND ASPECTS OF ACTIVE RC-FILTERS SYNTHESIS.
TH-Report 71-E-27. 1970. ISBN 90-6144-027-0

28) Boeschoten, F.
TWO FLUIDS MODEL REEXAMINED FOR A COLLISIONLESS PLASMA IN THE STATIONARY STATE.
TH-Report 72-E-28. 1972. ISBN 90-6144-028-9

EINDHOVEN UNIVERSITY OF TECHNOLOGY
THE NETHERLANDS
DEPARTMENT OF ELECTRICAL ENGINEERING

Reports:

29) REPORT ON THE CLOSED CYCLE MHD SPECIALIST MEETING. Working group of the joint ENEA/IAEA International MHD Liaison Group.
Eindhoven, The Netherlands, September 20-22, 1971. Edited by **L.H.Th. Rietjens.**
TH-Report 72-E-29. 1972. ISBN 90-6144-029-7

30) **Kessel, C.G.M. van and J.W.M.A. Houben**
LOSS MECHANISMS IN AN MHD GENERATOR.
TH-Report 72-E-30. 1972. ISBN 90-6144-030-0

31) **Veefkind, A.**
CONDUCTION GRIDS TO STABILIZE MHD GENERATOR PLASMAS AGAINST IONIZATION INSTABILITIES.
TH Report 72-E-31. 1972. ISBN 90-6144-031-9

32) **Daalder, J.E., and C.W.M. Vos**
DISTRIBUTION FUNCTIONS OF THE SPOT DIAMETER FOR SINGLE- AND MULTI-CATHODE DISCHARGES IN VACUUM.
TH-Report 73-E-32. 1973. ISBN 90-6144-032-7

33) **Daalder, J.E.**
JOULE HEATING AND DIAMETER OF THE CATHODE SPOT IN A VACUUM ARC.
TH-Report 73-E-33. 1973. ISBN 90-6144-033-5

34) **Huber, C.**
BEHAVIOUR OF THE SPINNING GYRO ROTOR.
TH-Report 73-E-34. 1973. ISBN 90-6144-034-3

35) **Bastian, C. et al.**
THE VACUUM ARC AS A FACILITY FOR RELEVANT EXPERIMENTS IN FUSION RESEARCH. Annual Report 1972. EURATOM-T.H.E. Group 'Rotating Plasma'.
TH-Report 73-E-35. 1973. ISBN 90-6144-035-1

36) **Blom, J.A.**
ANALYSIS OF PHYSIOLOGICAL SYSTEMS BY PARAMETER ESTIMATION TECHNIQUES.
TH-Report 73-E-36. 1973. ISBN 90-6144-036-X

37) **Cancelled**

38) **Andriessen, F.J., W. Boerman and I.F.E.M. Holtz**
CALCULATION OF RADIATION LOSSES IN CYLINDER SYMMETRIC HIGH PRESSURE DISCHARGES BY MEANS OF A DIGITAL COMPUTER.
TH-Report 73-E-38. 1973. ISBN 90-6144-038-6

39) **Dijk, J., C.T.W. van Diepenbeek, E.J. Maanders and L.F.G. Thurlings**
THE POLARIZATION LOSSES OF OFFSET ANTENNAS.
TH-Report 73-E-39. 1973. ISBN 90-6144-039-4

40) **Goes, W.P.**
SEPARATION OF SIGNALS DUE TO ARTERIAL AND VENOUS BLOOD FLOW IN THE DOPPLER SYSTEM THAT USES CONTINUOUS ULTRASOUND.
TH-Report 73-E-40. 1973. ISBN 90-6144-040-8

41) **Damen, A.A.H.**
A COMPARATIVE ANALYSIS OF SEVERAL MODELS OF THE VENTRICULAR DEPOLARIZATION; INTRODUCTION OF A STRING-MODEL.
TH-Report 73-E-41. 1973. ISBN 90-6144-041-6

EINDHOVEN UNIVERSITY OF TECHNOLOGY
THE NETHERLANDS
DEPARTMENT OF ELECTRICAL ENGINEERING

Reports:

42) **Dijk, G.H.M. van**
THEORY OF GYRO WITH ROTATING GIMBAL AND FLEXURAL PIVOTS.
TH-Report 73-E-42. 1973. ISBN 90-6144-042-4

43) **Breimer, A.J.**
ON THE IDENTIFICATION OF CONTINOUS LINEAR PROCESSES.
TH-Report 74-E-43. 1974. ISBN 90-6144-043-2

44) **Lier, M.C. van and R.H.J.M. Otten**
CAD OF MASKS AND WIRING.
TH-Report 74-E-44. 1974. ISBN 90-6144-044-0

45) **Bastian, C. et al.**
EXPERIMENTS WITH A LARGE SIZED HOLLOW CATHODE DISCHARDE FED WITH ARGON. Annual Report 1973. EURATOM-T.H.E. Group 'Rotating Plasma'.
TH-Report 74-E-45. 1974. ISBN 90-6144-045-9

46) **Roer, Th.G. van de**
ANALYTICAL SMALL-SIGNAL THEORY OF BARITT DIODES.
TH-Report 74-E-46. 1974. ISBN 90-6144-046-7

47) **Leliveld, W.H.**
THE DESIGN OF A MOCK CIRCULATION SYSTEM.
TH-Report 74-E-47. 1974. ISBN 90-6144-047-5

48) **Damen, A.A.H.**
SOME NOTES ON THE INVERSE PROBLEM IN ELECTRO CARDIOGRAPHY.
TH-Report 74-E-48. 1974. ISBN 90-6144-048-3

49) **Meeberg, L. van de**
A VITERBI DECODER.
TH-Report 74-E-49. 1974. ISBN 90-6144-049-1

50) **Poel, A.P.M. van der**
A COMPUTER SEARCH FOR GOOD CONVOLUTIONAL CODES.
TH-Report 74-E-50. 1974. ISBN 90-6144-050-5

51) **Sampic, G.**
THE BIT ERROR PROBABILITY AS A FUNCTION PATH REGISTER LENGTH IN THE VITERBI DECODER.
TH-Report 74-E-51. 1974. ISBN 90-6144-051-3

52) **Schalkwijk, J.P.M.**
CODING FOR A COMPUTER NETWORK.
TH-Report 74-E-52. 1974. ISBN 90-6144-052-1

53) **Stapper, M.**
MEASUREMENT OF THE INTENSITY OF PROGRESSIVE ULTRASONIC WAVES BY MEANS OF RAMAN-NATH DIFRACTION.
TH-Report 74-E-53. 1974. ISBN 90-6144-053-X

54) **Schalkwijk, J.P.M. and A.J. Vinck**
SYNDROME DECODING OF CONVOLUTIONAL CODES.
TH-Report 74-E-54. 1974. ISBN 90-6144-054-8

55) **Yakimov, A.**
FLUCTUATIONS IN IMPATT-DIODE OSCILLATORS WITH LOW Q-FACTORS.
TH-Report 74-E-55. 1974. ISBN 90-6144-055-6

EINDHOVEN UNIVERSITY OF TECHNOLOGY
THE NETHERLANDS
DEPARTMENT OF ELECTRICAL ENGINEERING

Reports:

56) **Plaats, J. van der**
ANALYSIS OF THREE CONDUCTOR COAXIAL SYSTEMS. Computer-aided determination of the frequency characteristics and the impulse and step response of a two-port consisting of a system of three coaxial conductors terminating in lumped impedances.
TH-Report 75-E-56. 1975. ISBN 90-6144-056-4

57) **Kalken, P.J.H. and C. Kooy**
RAY-OPTICAL ANALYSIS OF A TWO DIMENSIONAL APERTURE RADIATION PROBLEM.
TH-Report 75-E-57. 1975. ISBN 90-6144-057-2

58) **Schalkwijk, J.P.M., A.J. Vinck and L.J.A.E. Rust**
ANALYSIS AND SIMULATION OF A SYNDROME DECODER FOR A CONSTRAINT LENGTH k = 5, RATE R = ½ BINARY CONVOLUTIONAL CODE.
TH-Report 75-E-58. 1975. ISBN 90-6144-058-0.

59) **Boeschoten, F. et al.**
EXPERIMENTS WITH A LARGE SIZED HOLLOW CATHODE DISCHARGE FED WITH ARGON, II. Annual Report 1974. EURATOM-T.H.E. Group 'Rotating Plasma'.
TH-Report 75-E-59. 1975. ISBN 90-6144-059-9

60) **Maanders, E.J.**
SOME ASPECTS OF GROUND STATION ANTENNAS FOR SATELLITE COMMUNICATION.
TH-Report 75-E-60. 1975. ISBN 90-6144-060-2

61) **Mawira, A. and J. Dijk**
DEPOLARIZATION BY RAIN: Some Related Thermal Emission Considerations.
TH-Report 75-E-61. 1975. ISBN 90-6144-061-0

62) **Safak, M.**
CALCULATION OF RADIATION PATTERNS OF REFLECTOR ANTENNAS BY HIGH-FREQUENCY ASYMPTOTIC TECHNIQUES.
TH-Report 76-E-62. 1976. ISBN 90-6144-062-9

63) **Schalkwijk, J.P.M. and A.J. Vinck**
SOFT DECISION SYNDROME DECODING.
TH-Report 76-E-63. 1976. ISBN 90-6144-063-7

64) **Damen, A.A.H.**
EPICARDIAL POTENTIALS DERIVED FROM SKIN POTENTIAL MEASUREMENTS.
TH-Report 76-E-64. 1976. ISBN 90-6144-064-5

65) **Bakhuizen, A.J.C. and R. de Boer**
ON THE CALCULATION OF PERMEANCES AND FORCES BETWEEN DOUBLY SLOTTED STRUCTURES.
TH-Report 76-E-65. 1976. ISBN 90-6144-065-3

66) **Geutjes, A.J.**
A NUMERICAL MODEL TO EVALUATE THE BEHAVIOUR OF A REGENERATIVE HEAT EXCHANGER AT HIGH TEMPERATURE.
TH-Report 76-E-66. 1976. ISBN 90-6144-066-1

67) **Boeschoten, F. et al.**
EXPERIMENTS WITH A LARGE SIZED HOLLOW CATHODE DISCHARGE, III; concluding work Jan. 1975 to June 1976 of the EURATOM-THE Group 'Rotating Plasma'.
TH-Report 76-E-67. 1976. ISBN 90-6144-067-X

68) **Cancelled.**

EINDHOVEN UNIVERSITY OF TECHNOLOGY
THE NETHERLANDS
DEPARTMENT OF ELECTRICAL ENGINEERING

Reports:

69) **Merck, W.F.H. and A.F.C. Sens**
THOMSON SCATTERING MEASUREMENTS ON A HOLLOW CATHODE DISCHARGE.
TH-Report 76-E-69. 1976. ISBN 90-6144-069-6

70) **Jongbloed, A.A.**
STATISTICAL REGRESSION AND DISPERSION RATIOS IN NONLINEAR SYSTEM IDENTIFICATION.
TH-Report 77-E-70. 1977. ISBN 90-6144-070-X

71) **Barrett, J.F.**
BIBLIOGRAPHY ON VOLTERRA SERIES HERMITE FUNCTIONAL EXPANSIONS AND RELATED SUBJECTS.
TH-Report 77-E-71. 1977. ISBN 90-6144-071-8

72) **Boeschoten, F. and R. Komen**
ON THE POSSIBILITY TO SEPARATE ISOTOPES BY MEANS OF A ROTATING PLASMA COLUMN: Isotope separation with a hollow cathode discharge.
TH-Report 77-E-72. 1977. ISBN 90-6144-072-6

73) **Schalkwijk, J.P.M., A.J. Vinck and K.A. Post**
SYNDROME DECODING OF BINARY RATE-k/n CONVOLUTIONAL CODES.
TH-Report 77-E-73. 1977. ISBN 90-6144-073-4

74) **Dijk, J., E.J. Maanders and J.M.J. Oostvogels**
AN ANTENNA MOUNT FOR TRACKING GEOSTATIONARY SATELLITES.
TH-Report 77-E-74. 1977. ISBN 90-6144-074-2

75) **Vinck, A.J., J.G. van Wijk and A.J.P. de Paepe**
A NOTE ON THE FREE DISTANCE FOR CONVOLUTIONAL CODES.
TH-Report 77-E-75. 1977. ISBN 90-6144-075-0

76) **Daalder, J.E.**
RADIAL HEAT FLOW IN TWO COAXIAL CYLINDRICAL DISKS.
TH-Report 77-E-76. 1977. ISBN 90-6144-076-9

77) **Barrett, J.F.**
ON SYSTEMS DEFINED BY IMPLICIT ANALYTIC NONLINEAR FUNCTIONAL EQUATIONS.
TH-Report 77-E-77. 1977. ISBN 90-6144-077-7

78) **Jansen, J. and J.F. Barrett**
ON THE THEORY OF MAXIMUM LIKELIHOOD ESTIMATION OF STRUCTURAL RELATIONS. Part 1: One dimensional case.
TH-Report 78-E-78. 1977. ISBN 90-6144-078-5

79) **Borghi, C.A., A.F.C. Sens, A. Veefkind and L.H.Th. Rietjens**
EXPERIMENTAL INVESTIGATION ON THE DISCHARGE STRUCTURE IN A NOBLE GAS MHD GENERATOR.
TH-Report 78-E-79. 1978. ISBN 90-6144-079-3

80) **Bergmans, T.**
EQUALIZATION OF A COAXIAL CABLE FOR DIGITAL TRANSMISSION: Computer-optimized location of poles and zeros of a constant-resistance network to equalize a coaxial cable 1.2/4.4 for high-speed digital transmission (140 Mb/s).
TH-Report 78-E-80. 1978. ISBN 90-6144-080-7

EINDHOVEN UNIVERSITY OF TECHNOLOGY
THE NETHERLANDS
DEPARTMENT OF ELECTRICAL ENGINEERING

Reports:

81) **Kam, J.J. van der and A.A.H. Damen**
OBSERVABILITY OF ELECTRICAL HEART ACTIVITY STUDIES WITH THE SINGULAR VALUE DECOMPOSITION
TH-Report 78-E-81. 1978. ISBN 90-6144-081-5

82) **Jansen, J. and J.F. Barrett**
ON THE THEORY OF MAXIMUM LIKELIHOOD ESTIMATION OF STRUCTURAL RELATIONS. Part 2: Multi-dimensional case.
TH-Report 78-E-82. 1978. ISBN 90-6144-082-3

83) **Etten, W. van and E. de Jong**
OPTIMUM TAPPED DELAY LINES FOR THE EQUALIZATION OF MULTIPLE CHANNEL SYSTEMS.
TH-Report 78-E-83. 1978. ISBN 90-6144-083-1

83) **Vinck, A.J.**
MAXIMUM LIKELIHOOD SYNDROME DECODING OF LINEAR BLOCK CODES.
TH-Report 78-E-84. 1978. ISBN 90-6144-084-X

85) **Spruit, W.P.**
A DIGITAL LOW FREQUENCY SPECTRUM ANALYZER, USING A PROGRAMMABLE POCKET CALCULATOR.
TH-Report 78-E-85. 1978. ISBN 90-6144-085-8

86) **Beneken, J.E.W. et al**
TREND PREDICTION AS A BASIS FOR OPTIMAL THERAPY.
TH-Report 78-E-86. 1978. ISBN 90-6144-086-6

87) **Geus, C.A.M. and J. Dijk**
CALCULATION OF APERTURE AND FAR-FIELD DISTRIBUTION FROM MEASUREMENTS IN THE FRESNEL ZONE OF LARGE REFLECTOR ANTENNAS.
TH-Report 78-E-87. 1978. ISBN 90-6144-087-4

88) **Hajdasinski, A.K.**
THE GAUSS-MARKOV APPROXIMATED SCHEME FOR IDENTIFICATION OF MULTIVARIABELE DYNAMICAL SYSTEMS VIA THE REALIZATION THEORY.
An Explicit Approach.
TH-Report 78-E-88. 1978. ISBN 90-6144-088-2

89) **Niederlinski, A.**
THE GLOBAL ERROR APPROACH TO THE CONVERGENDE OF CLOSED-LOOP IDENTIFICATION, SELF-TUNING REGULATORS AND SELF-TUNING PREDICTORS.
TH-Report 78-E-89. 1978. ISBN 90-6144-089-0

90) **Vinck, A.J. and A.J.P. de Paepe**
REDUCING THE NUMBER OF COMPUTATIONS IN STACK DECODING OF CONVOLUTIONAL CODES BY EXPLOITING SYMMETRIES OF THE ENCODER.
TH-Report 78-E-90. 1978. ISBN 90-6144-090-4

91) **Geutjes, A.J. and D.J. Kleyn**
A PARAMETRIC STUDY OF 1000 MWe COMBINED CLOSED CYCLE MHD/STEAM ELECTRICAL POWER GENERATING PLANTS.
TH-Report 78-E-91. 1978. ISBN 90-6144-091-2

92) **Massee, P.**
THE DISPERSION RELATION OF ELECTROTHERMAL WAVES IN A NONEQUILIBRIUM MHD PLASMA.
TH-Report 78-E-92. 1978. ISBN 90-6144-092-0

EINDHOVEN UNIVERSITY OF TECHNOLOGY
THE NETHERLANDS
DEPARTMENT OF ELECTRICAL ENGINEERING

Reports:

93) Duin, C.A. van
DIPOLE SCATTERING OF ELECTROMAGNETIC WAVES PROPAGATION THROUGH A RAIN MEDIUM. TH-Report 79-E-93. 1979. ISBN 90-6144-093-9

94) Kuijper, A.H. de and L.K.J. Vandamme
CHARTS OF SPATIAL NOISE DISTRIBUTION IN PLANAR RESISTORS WITH FINITE CONTACTS. TH-Report 79-E-94. 1979. ISBN 90-6144-094-7